encyclopedia

MDPI

Review

Nonlocal Elasticity for Nanostructures: A Review of Recent Achievements

Raffaele Barretta *, Francesco Marotti de Sciarra and Marzia Sara Vaccaro

Department of Structures for Engineering and Architecture, University of Naples Federico II, via Claudio 21, 80125 Naples, Italy
* Correspondence: rabarret@unina.it

Abstract: Recent developments in modeling and analysis of nanostructures are illustrated and discussed in this paper. Starting with the early theories of nonlocal elastic continua, a thorough investigation of continuum nano-mechanics is provided. Two-phase local/nonlocal models are shown as possible theories to recover consistency of the strain-driven purely integral theory, provided that the mixture parameter is not vanishing. Ground-breaking nonlocal methodologies based on the well-posed stress-driven formulation are shown and commented upon as effective strategies to capture scale-dependent mechanical behaviors. Static and dynamic problems of nanostructures are investigated, ranging from higher-order and curved nanobeams to nanoplates. Geometrically nonlinear problems of small-scale inflected structures undergoing large configuration changes are addressed in the framework of integral elasticity. Nonlocal methodologies for modeling and analysis of structural assemblages as well as of nanobeams laying on nanofoundations are illustrated along with benchmark applicative examples.

Keywords: nonlocal continuum mechanics; nanostructures; integral elasticity

Citation: Barretta, R.; Marotti de Sciarra, F.; Vaccaro, M.S. Nonlocal Elasticity for Nanostructures: A Review of Recent Achievements. *Encyclopedia* **2023**, *3*, 279–310. https://doi.org/10.3390/encyclopedia3010018

Academic Editor: Stefano Falcinelli

Received: 1 February 2023
Revised: 16 February 2023
Accepted: 22 February 2023
Published: 27 February 2023

1. Introduction

According to traditional ideas in continuum mechanics, constitutive equations are those intrinsic relations providing response variables at a material point of a continuum as functions of variables assessed at the same point. Thus, classical constitutive laws support the axiom of local action, stating that response variables at a material point are not affected by the state of the continuum at distant material points. However, in determining the application field of local continuum mechanics, notion of length scale plays a crucial role. Indeed, if a continuum's external characteristic length (i.e., its structural dimension or wavelength) is significantly greater than its internal characteristic length (its interatomic distance or the size of its heterogeneities), then classical constitutive laws can accurately predict the outcome. In contrast, local theories are unable to capture the effective mechanical behavior if the external and internal characteristic lengths are comparable, and nonlocality thus becomes necessary to account for long-range interaction forces. According to nonlocal continuum field theories, constitutive response at a material point of a continuum depends on the state of all points and is thus characterized by response functionals [1,2].

Nowadays, modeling and optimization of smaller and smaller smart devices represent one of the most promising fields of application of nonlocal continuum mechanics due to the growing interest in nanoscience and nanotechnology. The development of mathematical tools able to capture size effects in small-scale structures has been pushed by the increasing attention to miniaturized electromechanical devices, with several potential applications in engineering science. In this regard, the main purpose consists of conceiving effective and computationally efficient methodologies to model size-dependent behavior and design small-scale structures exploiting unconventional tools provided by nonlocal continuum mechanics, rather than time-consuming atomistic approaches [3–5].

From the mathematical point of view, nonlocal theories provide enriched constitutive laws that are not pointwise and in which long distance interactions are described by internal characteristic lengths. In [6,7], Eringen developed one of the first theories of nonlocal integral elasticity, according to which stress is the convolution integral between the elastic strain field and a proper averaging kernel governed by an internal characteristic length. Such an integral theory is thus referred to as a strain-driven nonlocal theory, as proposed in [8]. Eringen's constitutive law has been efficiently adopted to solve screw dislocation and surface wave problems, but it turned out to be inconsistent when applied to structural problems due to an incompatibility between the constitutive law and equilibrium condition. Application of the strain-driven nonlocal model to structural mechanics led to alleged paradoxical results, as detected in [9,10] and definitely clarified by [11].

In order to address the issues related to the strain-driven nonlocal theory, several formulations have been conceived in recent years. Among these improved elasticity formulations, two-phase (local and nonlocal) mixture models stand out as a useful tool to overcome the ill-posedness of Eringen's theory and effectively capture scale-dependent mechanical behaviors. A two-phase model based on a convex combination of local and strain-driven integral responses was first proposed by Eringen in [12,13]. The mixture theory of elasticity was then restored in [14,15] to formulate well-posed structural problems, assuming that the local fraction of the two-phase law was not vanishing [11]. An alternative mixture theory to bypass difficulties of the strain-driven purely nonlocal law was proposed in [16], namely the strain difference-based nonlocal model of elasticity.

To account for scale effects in nanostructures, other possible theories assume that constitutive responses depend on both elastic strain fields and higher-order gradient strain fields. Eringen's differential law and the strain gradient model of elasticity were interestingly combined by Aifantis in [17–19]. Lim et al. coupled Eringen's nonlocal law with the strain gradient elasticity [20] to address wave propagation problems in unbounded domains, leading to a higher-order differential constitutive equation. In the framework of structural mechanics, the necessity of constitutive boundary conditions associated with the differential formulation of nonlocal gradient elasticity was inferred by Barretta and Marotti de Sciarra in [21,22], where the relevant differential constitutive problem was definitely established. The theory of elastic material surfaces conceived by Gurtin and Murdoch in [23] is another important tool for the modeling of nano-mechanical behaviors. In this framework, a combination of nonlocal integral elasticity and surface elasticity was recently provided in [24] to assess the size-dependent mechanics of nanostructures. Nonlocal mathematical models have also been proposed to capture non-conventional phenomena, such as electric polarization in ferroelectric materials [25], and to address diffusion problems in heterogeneous structures [26].

A total remedy to the issues related to the strain-driven nonlocal elasticity was definitely overcome by the stress-driven integral formulation conceived by Romano and Barretta in [27]. According to this theory, size-dependent mechanical behaviors can be modeled by a new nonlocal elastic law based on a stress-driven formulation that provides a consistent approach inside the integral elasticity framework. The nonlocal elastic strain field at a point of a continuum is given as convolution integral between the local elastic strain and a scalar averaging kernel. The relevant continuum problem is well posed, and size effects due to long range interactions can be effectively captured [28–31]. In [32], the stress-driven nonlocal elasticity was generalized to a two-phase (local/nonlocal) model that is able to capture both softening and stiffening elastic responses. Moreover, the mixture methodology based on the stress-driven approach is well posed for any local fraction. This theory has been successfully applied in recent contributions, such as in [33–35].

Nowadays, growing attention is being paid to modeling and design of ultra-small structural systems exploiting consistent methodologies of nonlocal continuum mechanics. A review on the topic was contributed in [36], in which nano-mechanical behavior is investigated by means of strain-driven-based formulations of nonlocal elasticity. A brief overview can be found in [37], where a collection of works concerning applications of

nonlocal theories is provided with a main reference to stress-driven formulations. In the present treatment, a comprehensive overview of new developments and outcomes in the framework of nonlocal continuum mechanics applied to nanostructures is provided. Starting from early formulations of nonlocal mechanics, recent theories of integral elasticity are illustrated and exploited to solve challenging problems of current nanotechnological interest. Innovative nonlocal methodologies to solve complex nanosystems are illustrated. A consistent approach to model nanobeams on nonlocal foundations is finally examined.

2. Eringen's Theory of Integral Elasticity

Pioneering works on nonlocal continuum mechanics were first contributed during the 20th century by Rogula [1,38], Kröner [2], Krumhansl [39] and Kunin [40]. Then, Eringen conceived an integral model of elasticity which was effectively applied to solve Rayleigh wave propagation and screw dislocation problems [6,7]. With reference to a three-dimensional continuum, Eringen's formulation is based on the idea that stress $\boldsymbol{\sigma}$ at a point $\boldsymbol{x}$ is output of a convolution integral between the elastic response to the local strain field $\boldsymbol{\varepsilon}^{el}$ and a proper attenuation function ϕ_λ described by a characteristic parameter $\lambda > 0$. Id est,

$$\boldsymbol{\sigma}(\boldsymbol{x}) = \int_\Omega \phi_\lambda(\boldsymbol{x} - \bar{\boldsymbol{x}}) \boldsymbol{E}(\bar{\boldsymbol{x}}) \boldsymbol{\varepsilon}^{el}(\bar{\boldsymbol{x}})\, d\Omega_{\bar{\boldsymbol{x}}}\,, \tag{1}$$

where $\boldsymbol{E}$ is the local elastic stiffness tensor field and $\boldsymbol{x}$ and $\bar{\boldsymbol{x}}$ are position vectors. The constitutive law in Equation (1) is referred to as strain-driven model since $\boldsymbol{\varepsilon}^{el}$ is the source field, and specifically, it represents a Fredholm integral equation of the first kind in the unknown elastic strain field. The symbol Ω adopted in Equation (1) denotes the actual body placement, and $d\Omega_{\bar{\boldsymbol{x}}}$ denotes that integration over Ω is performed with respect to the variable $\bar{\boldsymbol{x}}$.

In order to formulate the relevant nonlocal elastic problem of equilibrium, the stress field $\boldsymbol{\sigma}$ must satisfy the equilibrium differential equation, and the total strain field $\boldsymbol{\varepsilon}$, which is the sum of the elastic $\boldsymbol{\varepsilon}^{el}$ and non-elastic $\boldsymbol{\varepsilon}^{nel}$ strain fields, must fulfill the kinematic compatibility requirement. Hence, the integro-differential formulation based on Equation (1) is obtained as follows:

$$\begin{cases} div\, \boldsymbol{\sigma}(\boldsymbol{x}) = -\mathbf{b}(\boldsymbol{x})\,, \\ \boldsymbol{\sigma}(\boldsymbol{x}) = \displaystyle\int_\Omega \phi_\lambda(\boldsymbol{x} - \bar{\boldsymbol{x}}) \boldsymbol{E}(\bar{\boldsymbol{x}}) \boldsymbol{\varepsilon}^{el}(\bar{\boldsymbol{x}})\, d\Omega_{\bar{\boldsymbol{x}}}\,, \\ \boldsymbol{\varepsilon}(\boldsymbol{x}) = sym\, \nabla \mathbf{u}(\boldsymbol{x})\,, \end{cases} \tag{2}$$

where $\boldsymbol{x} \in \Omega$, $\mathbf{u}$ is the displacement field and $\mathbf{b}$ represents the body forces. It is worth noting that when formulating structural problems of nonlocal continua, equilibrium and kinematics do not depend on the scale under consideration. Indeed, it only affects the constitutive law that must properly account for the size effects. The averaging kernel ϕ_λ appearing in the integral constitutive law in Equation (1) is a scalar attenuation function described by a non-dimensional parameter $\lambda > 0$. Its physical dimension is $[L^{-3}]$, and the nonlocal parameter is defined as the ratio between the internal and external characteristic lengths. Moreover, the classical constitutive law of local elasticity can be recovered from Equation (1) for $\lambda \to 0^+$ at the internal points of Ω. A comprehensive analysis of the limit behaviors can be found in [41].

Let us start by applying Eringen's integral law to a one-dimensional model. Specifically, let us consider a Bernoulli–Euler beam of length L and take the abscissa x along the beam axis. By denoting with M the bending interaction field and with χ^{el} the elastic flexural curvature field, application of Eringen's theory leads to the following nonlocal elastic constitutive relation [42], id est

$$M(x) = \int_0^L \phi_\lambda(x - \bar{x})\,(k_f\,\chi^{el})(\bar{x})d\bar{x}\,, \tag{3}$$

where $k_f := I_E$ is the local elastic bending stiffness, (i.e., the second moment of the Euler–Young modulus field E on the beam cross-section). It is worth noting that the unknown elastic curvature is implicitly defined by Equation (3), since it is input of Eringen's convolution integral. As will be discussed in the following, solution of the integral Equation (3) in terms of elastic flexural curvature χ^{el} may not exist for an assigned output, provided by the bending interaction field fulfilling differential and boundary conditions of equilibrium.

2.1. Averaging Kernel and Green's Function

The attenuation kernel ϕ_λ can be chosen among Gaussian, exponential or power law function types. As suggested in [7], proper averaging kernels are represented by the Helmholtz bi-exponential function:

$$\phi_\lambda(x) = \frac{1}{2c}\exp\left(-\frac{|x|}{c}\right), \tag{4}$$

and by the normal distribution:

$$\phi_\lambda^{err}(x) = \frac{1}{c\sqrt{\pi}}\exp\left(-\frac{x^2}{c^2}\right), \tag{5}$$

where λ is defined as the ratio $\frac{c}{L}$, being c the internal characteristic length. Since the choice of different kernels leads to technically coincidental results [43], adoption of the bi-exponential function in Equation (4), as proposed by Eringen in [7], does not affect the generality but is more convenient from a theoretical and computational point of view. Indeed, the averaging function in Equation (4) is also called special kernel since it satisfies peculiar properties [11] that enable inversion of the constitutive integral equation.

Notably, the Helmholtz kernel $\phi_\lambda : \Re \to [0, +\infty[$ satisfies the following properties on the real axis:

- Symmetry and positivity

$$\phi_\lambda(x - \bar{x}) = \phi_\lambda(\bar{x} - x) \geq 0 \tag{6}$$

- Normalization

$$\int_{-\infty}^{+\infty} \phi_\lambda(x)\,dx = 1 \tag{7}$$

- Limit impulsivity

$$\lim_{\lambda \to 0^+} \int_{-\infty}^{+\infty} \phi_\lambda(x - \bar{x})\,f(\bar{x})d\bar{x} = f(x) \tag{8}$$

  for any continuous function $f : \Re \to \Re$.

As proven in [27], the following proposition holds:

Proposition 1. *The Helmholtz kernel ϕ_λ is Green's function associated with the differential operator $1 - c^2\,\partial_x^2$ and satisfying the boundary conditions*

$$\begin{cases} \partial_x\phi_\lambda(0) = \dfrac{1}{c}\phi_\lambda(0)\,, \\ \partial_x\phi_\lambda(L) = -\dfrac{1}{c}\phi_\lambda(L)\,, \end{cases} \tag{9}$$

where symbol ∂_x in Equation (9) denotes derivative along the x axis. For decreasing values of λ, the kernel's support reduces, and the peak of the function increases while, for increasing λ values, more and more abscissae of the domain are involved in the convolution

integral, thus increasing the propagation of long-range interactions. It is worth noting that the limit impulsivity property in Equation (8) is defined on the real axis. For bounded domains (e.g., the interval $[a,b]$ with $a,b \in \Re$), the property can be reformulated as shown below. First, let us introduce the following function:

$$\Theta(x) = \begin{cases} 1, & x \in]a,b[\,, \\ 1/2, & x = \{a,b\}\,. \end{cases} \tag{10}$$

Then, the impulsivity property in a bounded domain can be rewritten as

$$\lim_{\lambda \to 0^+} \int_a^b \phi_\lambda(x-\bar{x})\, f(\bar{x}) d\bar{x} = \Theta(x)\, f(x) \tag{11}$$

for any continuous real scalar function f. Equation (11) states that the Helmholtz function for $\lambda \to 0^+$ is the Dirac delta or the halved Dirac delta if the abscissa of evaluation is internal or external to the domain [11]; that is, for $x \in]a,b[$, in the limit, the source field $f(x)$ is found as the output of the convolution integral, while for $x = \{a,b\}$, we find the halved response $f(x)/2$. This boundary effect is caused by the fact that the kernel's support exceeds the structural domain at the exterior boundary. Therefore, in the limit for $\lambda \to 0^+$, the local constitutive law of elasticity is recovered at the interior abscissae.

As stated before, the Helmholtz function ϕ_λ satisfies the peculiar properties that enable inversion of the integral law to obtain an equivalent differential problem of Eringen's model in Equation (3), which is expressed by the following proposition:

Proposition 2. *For any $\lambda > 0$, the integral constitutive law*

$$M(x) = \int_a^b \phi_\lambda(x-\bar{x})\, (k_f\, \chi^{el})(\bar{x}) d\bar{x} \tag{12}$$

equipped with the bi-exponential kernel in Equation (4) admits either a unique solution or no solution at all, depending on whether or not the following constitutive boundary conditions are satisfied by the equilibrated bending interaction field

$$\begin{cases} \partial_x M(a) = \dfrac{1}{c} M(a)\,, \\ \partial_x M(b) = -\dfrac{1}{c} M(b)\,. \end{cases} \tag{13}$$

If Equation (13) is fulfilled by the equilibrated bending interaction field, then the unique solution χ^{el} is obtained from the second order differential equation

$$M(x) - c^2\, \partial_x^2 M(x) = k_f(x)\, \chi^{el}(x)\,. \tag{14}$$

Therefore, an equivalent differential problem is provided to explicitly find the unknown field χ^{el}. Moreover, the differential formulation represents a direct tool to detect if the Fredholm integral equation of the first kind represented by Equation (12) admits solution for an assigned output field M fulfilling the equilibrium requirements. Indeed, a unique elastic curvature χ^{el} can be found if and only if the constitutive boundary conditions in Equation (13) are fulfilled by the equilibrated bending interaction field. Otherwise, no solution exists.

Several scientific contributions have been proposed by adopting the constitutive differential law in Equation (14) without prescription of constitutive boundary conditions in Equation (13), whose necessity was first inferred in [42,44]. Paradoxical cases have been detected by applying Eringen's differential law to structural problems. The question has been definitely clarified in [45], where inconsistency of the strain-driven nonlocal

formulation was shown. The constitutive boundary conditions in Equation (13) indeed relate the bending and shearing interaction fields at the boundary for any value of the characteristic length, and thus they are, in general, in contrast with the natural boundary conditions. Thus, there is a lack of solution existence due to the fact that the integral constitutive law is incompatible with equilibrium requirements.

2.2. The Alleged Paradox of the Nonlocal Elastic Cantilever

Eringen's differential law in Equation (14) has been widely applied to structural problems, disregarding the prescription of boundary conditions in Equation (13). Accordingly, application of Eringen's differential model to small-scale cantilevers under concentrated loading at the free end led to an alleged paradoxical case, as first detected by Peddieson in [9] and then by Challamel in [10]. After the discussions provided in [42,44], explanation of the paradoxical results was finally proposed in [45]. The alleged paradoxical case is discussed here. For the structural problem under consideration, the bending interaction field is univocally determined by differential and boundary conditions of equilibrium; that is, $M(x) = \mathcal{F}(L - x)$. By applying Eringen's differential law in Equation (14), we obtain

$$M(x) = k_f(x)\,\chi^{el}(x)\,, \tag{15}$$

that is, the nonlocal constitutive model collapses into the local law, and accordingly, no size effects arise. Moreover, accounting for Equation (15) in the strain-driven convolution integral in Equation (12) leads to

$$M(x) = \int_0^L \phi_\lambda(x - \bar{x})\,\mathcal{F}(L - \bar{x})d\bar{x}\,. \tag{16}$$

The output of Equation (16) provides the following bending interaction that is a nonlinear field:

$$M(x) = \frac{1}{2}\mathcal{F}\,L\left(\lambda \exp\left(\frac{x-L}{c}\right) - (1+\lambda)\exp\left(-\frac{x}{c}\right) + 2\left(1 - \frac{x}{L}\right)\right) \tag{17}$$

which does not fulfill the differential and boundary conditions of equilibrium. Such a result has been considered a paradoxical case, but the proper interpretation is that the strain-driven integral law does not have solution. Indeed, according to Proposition 2, the equilibrated bending interaction field cannot fulfill the constitutive boundary conditions shown below:

$$\begin{cases} -\mathcal{F} = \dfrac{1}{c}\mathcal{F}\,L\,, \\ -\mathcal{F} = 0\,. \end{cases} \tag{18}$$

As emerged from Equation (18), the boundary conditions can be satisfied only for a vanishing applied concentrated loading that is of no applicative interest. Therefore, the relevant nonlocal problem is ill-posed due to the incompatibility between the constitutive law and equilibrium conditions.

Figures 1–3 represent the bending and shearing interactions fields and the emerging loading fields, respectively, revealing that the equilibrium requirements are clearly violated. This pathological behavior concerns all nonlocal structural problems of applicative interest, as shown in [45].

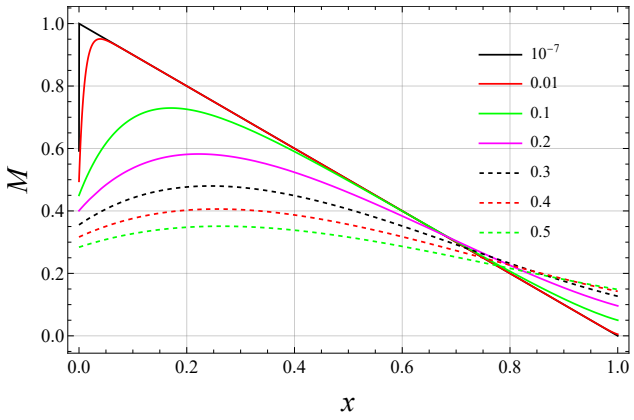

Figure 1. Bending interaction field as function of λ.

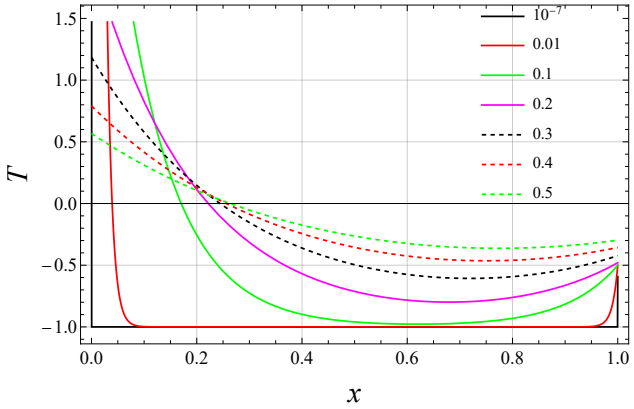

Figure 2. Shearing interaction field as function of λ.

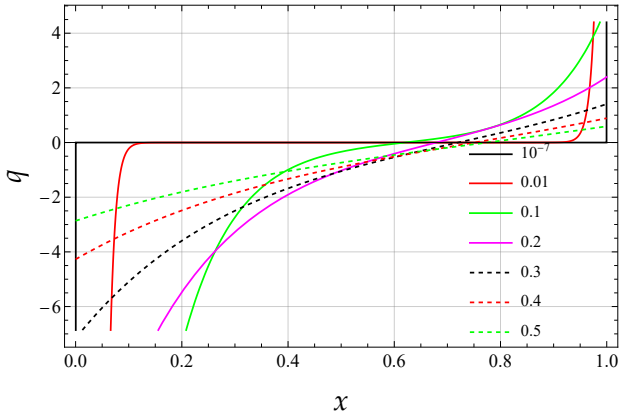

Figure 3. Emerging loading field as function of λ.

3. Strain-Driven Nonlocal Methodologies

To overcome the issues emerging from the application of the strain-driven model, a mixture model of elasticity was proposed by Eringen in [12] and then restored in [14,15]. Eringen's two-phase model was proposed in [46] for buckling analysis of slender beams, free vibration analyses of Euler–Bernoulli curved beams have been performed in [47], post-buckling of viscoelastic nanobeams has been analysed in [48], bending problem of two-phase elastic structures has been addressed in [49], mixture nonlocal integral theories have been adopted in [50] for functionally graded Timoshenko beams.

With reference to an inflected beam, Eringen's two-phase theory expresses the bending interaction field as a convex combination of the local and nonlocal responses by means

of a mixture parameter. Since the mixture model is a two-parameter theory, it provides a generalization of the purely strain-driven nonlocal model and thus is able to capture the size-dependent behavior of a wide class of applications. According to the two-phase strain-driven theory, the bending interaction field M is a convex combination of the local response $s := k_f\,\chi^{el}$ and the convolution integral between the local source field s and the attenuation function ϕ_λ, id est

$$M(x) = \alpha\, s(x) + (1-\alpha)\int_0^L \phi_\lambda(x-\xi)\, s(\xi)\, d\xi\,, \tag{19}$$

where α is the mixture parameter $0 \le \alpha \le 1$ and $\lambda > 0$ is the nonlocal parameter describing the averaging kernel. For $\alpha = 0$, the purely nonlocal response is got $M(x) = \int_0^L \phi_\lambda(x-\xi)\,(k_f\,\chi^{el})(\xi)\, d\xi$ while for $\alpha = 1$, the local case $M = k_f\,\chi^{el}$ is recovered. It is worth noting that Equation (19) represents a Fredholm integral equation of the second kind in the unknown source field s (see [51,52]).

If the special kernel is adopted, then an equivalent differential problem can be derived [11]:

$$\frac{M(x)}{c^2} - \partial_x^2 M(x) = \frac{(k_f\,\chi^{el})(x)}{c^2} - \alpha\,\partial_x^2 (k_f\,\chi^{el})(x)\,, \tag{20}$$

$$\begin{cases} \partial_x M(0) - \dfrac{1}{c}\,M(0) = \alpha\left(\partial_x (k_f\,\chi^{el})(0) - \dfrac{(k_f\,\chi^{el})(0)}{c}\right), \\ \partial_x M(L) + \dfrac{1}{c}\,M(L) = \alpha\left(\partial_x (k_f\,\chi^{el})(L) + \dfrac{(k_f\,\chi^{el})(L)}{c}\right). \end{cases} \tag{21}$$

The strain-driven two-phase model provides a well-posed structural problem only for a strictly positive mixture parameter $\alpha > 0$, while for $\alpha = 0$, the purely integral Eringen's law is recovered.

An alternative theory to bypass the ill-posedness of the strain-driven fully integral formulation was proposed in [16], namely the strain difference-based nonlocal elasticity model. This constitutive theory was conceived on the basis of the so-called "locality recovery condition"; that is, the nonlocal stress response is required to be uniform if the source local strain is uniform. A critical analysis of locality recovery can be found in [53]. Fulfillment of the above-mentioned requirement leads to the following constitutive local/nonlocal integral law:

$$M(x) = \Big(1-\gamma(x)\Big)\,(k_f\,\chi^{el})(x) + \int_0^L \phi_\lambda(x-\xi)\,(k_f\,\chi^{el})(\xi)\, d\xi\,, \tag{22}$$

where the function γ is defined as the integral of the attenuation kernel over the domain (i.e., $\gamma(x) := \int_0^L \phi_\lambda(x-\xi)\, d\xi$) such that Equation (22) can also be rewritten as follows:

$$M(x) = (k_f\,\chi^{el})(x) + \int_0^L \phi_\lambda(x-\xi)\,\Big((k_f\,\chi^{el})(\xi) - (k_f\,\chi^{el})(x)\Big)\, d\xi\,. \tag{23}$$

The latter form clarifies the strain difference appellation given to this elasticity theory. It is worth noting that for decreasing λ values, the function $1-\gamma(x)$ is vanishing in a non-empty core domain such that the model tends to collapse into the purely nonlocal strain-driven theory. A correction to this drawback was proposed in [54] by modifying Equation (22) as follows:

$$M(x) = \beta(x)\,(k_f\,\chi^{el})(x) + \int_0^L \phi_\lambda(x-\xi)\,(k_f\,\chi^{el})(\xi)\, d\xi\,, \tag{24}$$

where $\beta(x) := e + 1 - \gamma(x)$ being $e \ll 1$ a constant corrective factor. Equation (24) still represents a Fredholm integral equation of the second kind in the unknown field of the elastic curvature.

Among the strain-driven nonlocal methodologies, a recent contribution was provided in [55], in which the differential law in Equation (14) was reconsidered to predict the size effects in small-scale beams. It is important to underline that the differential law, without prescription of the constitutive boundary conditions, is not equivalent to Eringen's integral nonlocal theory. Thus, the differential model provided by Equation (14) represents a local constitutive law of elasticity that differs from the classical one for the term $-c^2\,\partial_x^2 M(x)$, which accounts for size effects and can be rewritten as $-c^2\,q(x)$ by exploiting the differential equilibrium condition of the Bernoulli–Euler beam theory. Equation (14) can be rewritten as $M(x) = k_f\big(\chi(x) - \chi^{nel}(x)\big)$, where the term taking into account the size effects $\chi^{nel}(x) := -\dfrac{c^2}{k_f}\,q(x)$ is interpreted as a fictitious non-elastic curvature. This latter term was modified in [55] by including both reactive and active distributed and concentrated loadings, id est

$$\chi^{nel}(x) := -\frac{c^2}{k_f}\left(q(x) + \sum_{i=1}^{n} \mathcal{F}_i\,\delta(x - x_i) + R_0\,\delta(x) + R_L\,\delta(x - L)\right) \tag{25}$$

where $\mathcal{F}_i$ is the ith concentrated force, R_0, R_L represents the reactive forces and n is the number of concentrated loadings. The proposed differential model may not be able to capture long-range interactions in general structural problems. An exemplar case is provided by a simple cantilever under a concentrated couple, for which the fictitious non-elastic curvature is zero and thus no size effects arise.

4. The Stress-Driven Nonlocal Model

To completely overcome the ill-posedness of strain-driven formulations, a consistent theory was proposed in [27], obtained by swapping the roles of stress and elastic strain in Equation (1) to find a stress-driven integral law which is not the inverse of the previous one. The stress-driven methodology has been effectively applied to study the scale effects in axisymmetric nanoplates [56], to investigate size-dependent bending problems [57], to examine the buckling of nanobeams [58], to address vibration problems in nanorods [59], to perform nonlinear dynamic analyses of functionally graded porous nanobeams [60], to model carbon nanotubes conveying magnetic nanoflow [61] and to analyze the size-dependent buckling problems of cracked micro- and nano-cantilevers [62].

With reference to a three-dimensional continuum, the stress-driven nonlocal model is written as follows:

$$\boldsymbol{\varepsilon}^{el}(\boldsymbol{x}) = \int_{\Omega} \phi_\lambda(\boldsymbol{x} - \bar{\boldsymbol{x}})\boldsymbol{C}(\bar{\boldsymbol{x}})\boldsymbol{\sigma}(\bar{\boldsymbol{x}})\,d\Omega_{\bar{\boldsymbol{x}}}\,, \tag{26}$$

where $\boldsymbol{C} := \boldsymbol{E}^{-1}$ is the elastic compliance tensor field. The constitutive integral Equation (26) explicitly expresses the elastic strain $\boldsymbol{\varepsilon}^{el}$ as a convolution integral between the averaging kernel and the stress field $\boldsymbol{\sigma}$. The stress field $\boldsymbol{\sigma}$ must satisfy the equilibrium requirements, while the geometric strain field $\boldsymbol{\varepsilon}$, sum of the elastic and non-elastic strain fields, must fulfill the kinematic compatibility requirement.

Applied to a slender beam of length $L := b - a$, the integral law in Equation (26) is written as follows:

$$\chi^{el}(x) = \int_a^b \phi_\lambda(x - \bar{x})\,(k_f^{-1}\,M)(\bar{x})d\bar{x}\,, \tag{27}$$

where k_f^{-1} is the elastic flexural compliance. It is useful to note that according to the strain-driven model in Equation (12), the bending interaction field is expressed as

$$M(x) = \Big(\phi_\lambda\ *\,(k_f\,\chi^{el})\Big)(x)\,, \tag{28}$$

where $\phi_\lambda *$ is the linear convolution operator. Thus, the strain-driven law in Equation (28) provides an implicit definition of the unknown elastic curvature field χ^{el}, and it represents a Fredholm integral equation of the first kind, which is known to generally lead to no solution at all or to multiple solutions. Conversely, in the stress-driven formulation, the operator $\phi_\lambda *$ is directly applied to the equilibrated bending interaction field to explicitly find the nonlocal elastic curvature:

$$\chi^{el}(x) = \left(\phi_\lambda * (k_f^{-1} M)\right)(x). \tag{29}$$

By virtue of the properties of the special kernel in Equation (4), the following equivalence can be stated. The nonlocal elastic curvature found by the stress-driven convolution integral

$$\chi^{el}(x) = \int_a^b \phi_\lambda(x - \bar{x})\,(k_f^{-1} M)(\bar{x}) d\bar{x} \tag{30}$$

provides the unique solution of the differential problem made of the second-order differential equation

$$\chi^{el}(x) - c^2\,\partial_x^2 \chi^{el}(x) = (k_f^{-1} M)(x), \tag{31}$$

equipped with the constitutive boundary conditions

$$\begin{cases} \partial_x \chi^{el}(a) = \dfrac{1}{c}\chi^{el}(a), \\ \partial_x \chi^{el}(b) = -\dfrac{1}{c}\chi^{el}(b). \end{cases} \tag{32}$$

The solution in terms of the elastic curvature is unique, since the corresponding homogeneous differential problem admits only the trivial solution. According to the stress-driven nonlocal model, the relevant structural problem is well-posed since no conflict arises with equilibrium conditions. Moreover, there is no incompatibility with the kinematic boundary conditions, since the constitutive boundary conditions in Equation (32) involve only the elastic curvature field and its first derivative. This is a fundamental requirement for a constitutive law, since it must be independent of the prescribed kinematic constraints.

A basic example is provided below concerning a doubly clamped beam under uniformly distributed loading whose size-dependent behavior is modeled by the stress-driven nonlocal approach. Figure 4 shows the maximum transverse displacement adimensionalized with respect to the maximum local response versus the nonlocal parameter. The structural response exhibits a stiffening effect for increasing λ values, in agreement with the outcomes collected in [63].

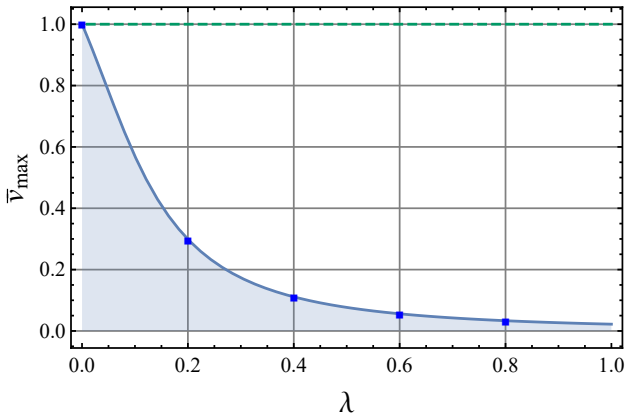

Figure 4. Clamped beam's maximum non-dimensional displacement versus nonlocal parameter.

This peculiar trend is due to the properties of the special kernel since the peak of the attenuation function reduces for increasing nonlocal parameter values, causing a decrease in

elastic flexural compliance, which has a predominant effect on the extension of the kernel's support. This feature is known as the "smaller-is-stiffer" phenomenon [64], characterizing a huge class of problems in nanoengineering.

Nonlinear Mechanics of Nonlocal Elastic Beams

Recent achievements in the field of nonlocal elasticity concern the modeling of nanostructures undergoing large configuration changes. Geometrically nonlinear analysis of Timoshenko nanobeams based on the strain-driven approach was carried out in [65], the nonlinear coupled mechanics of composite nanostructures were investigated in [66], the nonlinear dynamics of carbon nanotube-based mass sensors were studied in [67], the nonlinear vibration response of nanobeams was detected in [68] by exploiting Eringen's model, nonlinear dynamic analyses of graphene sheets were carried out in [69], the geometrically nonlinear bending problem of nanobeams was explored in [70], the nonlinear behaviors in nonlocal elastic shells were modeled in [71], the post-buckling of nanotubes was addressed in [72], the nonlinear vibrations of microbeams were examined in [73], nonlinear post-buckling analysis of functionally graded Timoshenko nonlocal beams was carried out in [74], large deflection analysis of a nano-cantilever on a Winkler–Pasternak foundation was performed in [75], and thermal buckling of piezomagnetic small-scale beams was studied in [76].

In [77], the stress-driven nonlocal elasticity was efficiently applied to capture size effects in small-scale beams undergoing large configuration changes. Based on the outcomes contributed in [77], a consistent stress-driven methodology of integral elasticity is shown in this section to address applicative problems of small-scale beams characterized by geometrically nonlinear behaviors. For this purpose, let us consider a nonlocal elastic cantilever of length L whose initial configuration is characterized by a null geometric flexural curvature. The beam is subjected to a concentrated loading $\mathcal{F}$ at the free end [77], and it is parameterized as $\mathbf{r} = \{x(s), y(s)\} = \{x, y(x)\}$, where $\mathbf{r}$ is the position vector and $s \in [0, L]$ is the curvilinear abscissa. The field of the tangent unit vectors is obtained as $\mathbf{t} := \partial_s \mathbf{r}$, and its derivative $\partial_s \mathbf{t}$ is the curvature vector, whose modulus provides the exact geometric curvature, id est

$$\chi(x) = \frac{\partial_x^2 y(x)}{\left[1 + \left(\partial_x y(x)\right)^2\right]^{3/2}}, \tag{33}$$

which is coincident with the elastic one, $\chi = \chi^{el}$, since inelastic effects are not considered. Exploiting the stress-driven theory, the flexural curvature can be got as

$$\chi(x) = \int_0^l \phi_\lambda(x - \xi) \left(\frac{M}{k_f}\right)(\xi)\, d\xi, \tag{34}$$

where l is the orthogonal projection of the end point along the x axis. In Equation (34), $M = \mathcal{F}(l - x)$ is the linear bending interaction field satisfying the equilibrium requirements. By making the change of variable $z := \partial_x y$ and integrating Equation (33), we obtain

$$G(x) = \int_0^x \chi(\eta) d\eta, \tag{35}$$

where the position $G := \dfrac{z}{\sqrt{1 + z^2}}$ has been done and the boundary condition $z(0) = 0$ has been prescribed. Taking into account $G := \partial_s y$ and $|\mathbf{t}| = \sqrt{\left(\partial_s x\right)^2 + G^2} = 1$, we finally obtain the differential equation in the unknown function $s(x)$, that is

$$\partial_x s(x) = \frac{1}{\sqrt{1 - G^2(x)}}, \text{ with } s(0) = 0. \tag{36}$$

Finally, the unknown length l is obtained by prescribing $s(l) = L$, and the current beam configuration $y(x)$ is got from

$$\partial_x y(x) = \frac{G(x)}{\sqrt{1 - G^2(x)}}, \text{ with } y(0) = 0. \tag{37}$$

The nonlinear problem of nonlocal elastic equilibrium described above is solved by performing an iterative solution procedure, which provides a generalization of the contribution [78] to the framework of integral elasticity. Starting from a trial projection length, l is updated at each step until the condition $s(l) = L$ is satisfied. The beam length is assumed to be $L = 100\,[\mu m]$ with a rectangular cross-section of height $5\,[\mu m]$ and base $3.5\,[\mu m]$. The Euler–Young modulus is $E = 80\,[GPa]$. Parametric analyses are performed to investigate the influence of nonlocal parameter λ and applied force $\mathcal{F}$. The results are represented in Figure 5, showing that structural responses exhibited a stiffening behavior for increasing λ values.

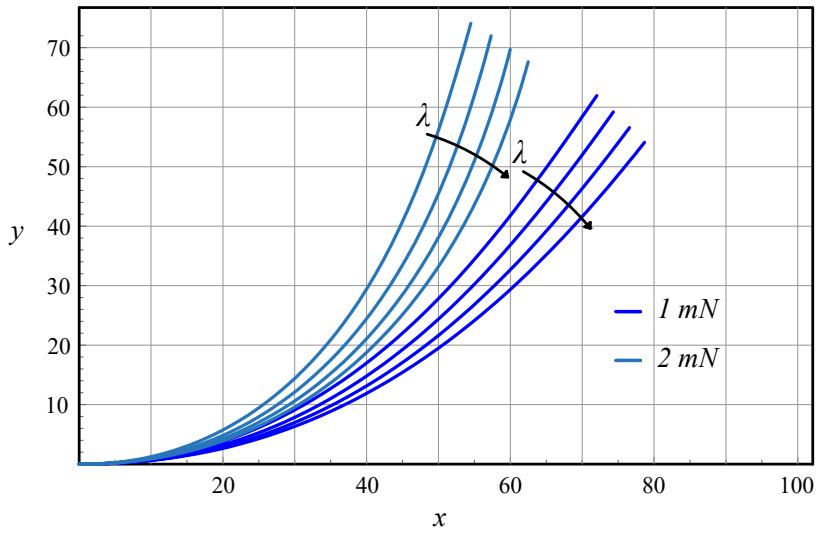

Figure 5. Current configuration $y\,[\mu m]$ of beam axis versus $x\,[\mu m]$ for $\lambda = \{0.05, 0.10, 0.15, 0.20\}$.

5. A Nonlocal Methodology for Shear Deformation Beam Theories

The stress-driven integral elasticity can be exploited to capture size-dependent behaviors of nonlocal beams whose kinematics is modeled by adopting higher-order kinematic theories [79–82]. By making reference to a three-dimensional Cauchy continuum shaped as a right prism of length L with cross-section Ω, the following vector field describes the kinematics according to the third-order theory [83,84]

$$\mathbf{u}(x, y, z) = \left[-y\,\varphi(x) - a\,y^3 \left(w'(x) - \varphi(x) \right) \right] \mathbf{i} + w(x)\mathbf{j} \tag{38}$$

where $\mathbf{i}$ is the unit vector directed along the x axis (the locus of the cross-sectional geometric centroids), while the y and z axes define the cross-sectional plane and are identified by the unit vectors $\mathbf{j}$ and $\mathbf{k} := \mathbf{i} \times \mathbf{j}$. In Equation (38), $w(x)$ is the transverse displacement field, and $\varphi(x)$ is defined such that $\varphi := -\left.\dfrac{\partial u_x}{\partial y}\right|_{y=0}$, while the coefficient a is $4/(3h^2)$, where h is the maximum cross-sectional dimension along the y axis. Starting from Equation (38), the following tangent deformation fields can be derived for the third-order

beam: $\{\bar{\varepsilon}, \bar{\gamma}, \bar{\bar{\varepsilon}}, \bar{\bar{\gamma}}\} = \{\varphi', w' - \varphi, a\,\bar{\gamma}', -b\,\bar{\gamma}\}$, where $b = 3\,a$. Then, prescription of the variational equilibrium condition [85] leads to the differential system

$$\begin{cases} b\,R'(x) - Q'(x) + a\,P''(x) = q(x)\,, \\ a\,P'(x) - M'(x) + b\,R(x) - Q(x) = 0\,, \end{cases} \tag{39}$$

equipped with the boundary conditions

$$\begin{cases} \big(Q - b\,R - a\,P'\big)(x_i)\,\delta w(x_i) = (-1)^i\,\mathcal{F}_i\,\delta w(x_i)\,, \\ P(x_i)\,\delta w'(x_i) = (-1)^i\,\mathcal{P}_i\,\delta w'(x_i)\,, \\ \big(M - a\,P\big)(x_i)\,\delta\varphi(x_i) = (-1)^i\,\mathcal{M}_i\,\delta\varphi(x_i)\,, \end{cases} \tag{40}$$

where $i = \{1, 2\}$, $x_1 := 0$ and $x_2 := L$. In Equation (40), δw, $\delta\varphi$, $\delta w'$ are virtual kinematic fields fulfilling the homogeneous kinematic boundary conditions, $\mathcal{F}_i$, $\mathcal{M}_i$ are concentrated forces and couples, and $\mathcal{P}_i$ represents the higher-order concentrated couples, while in Equation (39), q is the distributed transverse loading. Moreover, M and Q are the bending and shearing interaction fields, respectively, while P and R are the higher-order stress resultants. By following the approach proposed in [27], it can be proven that exploiting the stress-driven integral theory of elasticity, a constitutive system can be derived that is made of two convolution integral laws

$$\begin{cases} \bar{\varepsilon}(x) = \displaystyle\int_0^L \phi_\lambda(x-\xi)\left(\frac{M(\xi)}{I_E} - \frac{a\,I_E^{(4)}\,Q'(\xi)}{\bar{A}_G I_E}\right) d\xi\,, \\ \bar{\gamma}(x) = \displaystyle\int_0^L \phi_\lambda(x-\xi)\,\frac{Q(\xi)}{\bar{A}_G}\,d\xi\,, \end{cases} \tag{41}$$

and two elastic relations involving only stress fields:

$$\begin{cases} P(x) = \dfrac{I_E^{(4)}}{I_E}\left(M(x) - a\,\dfrac{I_E^{(4)}}{\bar{A}_G}Q'(x)\right) + a\,\dfrac{I_E^{(6)}}{\bar{A}_G}Q'(x)\,, \\ R(x) = \dfrac{\bar{I}_G^{(2)}}{\bar{A}_G}Q(x)\,, \end{cases} \tag{42}$$

where all functional dependencies among the tangent deformation fields have been taken into account. The equivalent differential formulation, which is useful for theoretical and computational purposes, can be found in [43], where an analytical procedure is proposed to obtain well-posed structural problems. A simply supported nanobeam under uniformly distributed loading $q = 5\,[nN/nm]$ is analyzed here. A silicon carbide beam with a Euler–Young modulus $E = 380\,[GPa]$ and Poisson's ratio $\nu = 0.3$ is examined [86]. The beam length is $L = 100\,[nm]$, and a rectangular cross-section is assumed with a height of $0.5\,L$ and base of $30\,[nm]$. From the boundary conditions in Equation (40), the pinned ends require $w(x_i) = P(x_i) = M(x_i) = 0$ for $i = \{1, 2\}$.

Parametric solutions in terms of shape functions w and φ are represented in Figures 6 and 7, showing stiffening responses for increasing non-dimensional nonlocal parameter λ. Solutions to the corresponding local structural problem are recovered for $\lambda \to 0^+$. Starting from the general third-order theory, mathematical formulation of the nonlocal structural problem based on the Timoshenko beam model can be recovered as a particular case by setting $a = 0$ in Equation (38). Solutions to the relative elastostatic problem can be found in [87]. It is worth noting that the outcomes contributed in [43] amend the erroneous statements in [88] regarding the ill-posed nature of the structural problem of third-order beams based on the stress-driven nonlocal model.

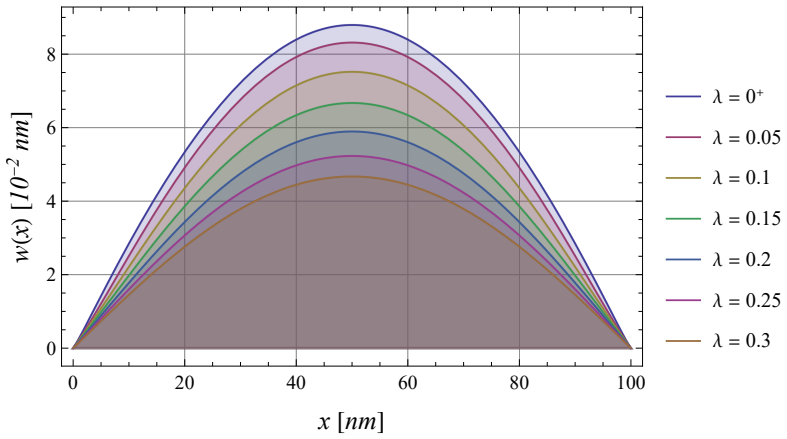

Figure 6. Simply supported beam under uniformly distributed loading: shape function w versus x.

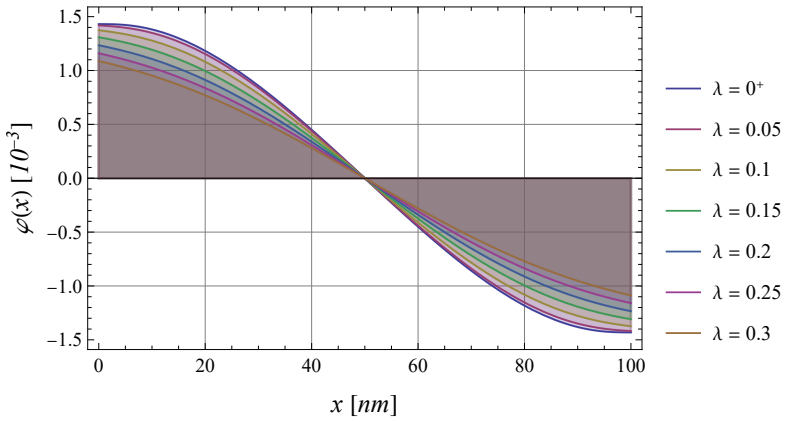

Figure 7. Simply supported beam under uniformly distributed loading: shape function φ versus x.

6. Stress-Driven Two-Phase Elasticity

Two-phase models of elasticity can be formulated by following the approach proposed in [11], providing a generalization of the stress-driven purely integral theory. Such a model leads to well-posed structural continuum problems for any value of the mixture parameter and has been effectively applied to capture the size-dependent behaviors of nanostructures, such as bending of nanobeams [32], fracture analysis of nonlocal continua [89], composite nanostructures in vibration [90], elastostatics of stubby curved nanobeams [33] and size-dependent mechanics of Bernoulli–Euler cracked nanobeams [91]. According to the stress-driven two-phase elasticity, the nonlocal response f is convex combination by means of the mixture parameter α of the local source field s and of the purely stress-driven convolution integral $\phi_\lambda * s$.

6.1. Two-Phase Elasticity for Stubby Curved Beams

The stress-driven two-phase elasticity is illustrated here with reference to curved stubby beams [33], whose kinematics is modeled by the Timoshenko theory. The treatment proposed in [33] provides a generalization of the outcomes contributed in [28] in which nonlocal mechanics of curved slender nanobeams is investigated by exploiting the stress-driven integral model and adopting a coordinate-free formulation. Moreover, particular solutions for vanishing mixture parameter can be found in [34], where Timoshenko curved beams are modeled by exploiting the purely stress-driven integral elasticity. Further contributions on the topic can be found in [92], in which nonlinear mechanics of curved nanobeams is addressed, in [93] where the time-dependent behavior of porous curved nanobeams is modeled, and in [94] where free vibration analysis of curved zigzag nanobeams is conducted.

In order to investigate the mechanics of curved nonlocal continua, the beam axis is assumed to be a regular planar curve $\mathbf{\Gamma}$ parameterized by the curvilinear abscissa $s \in [0, L]$ such that the tangent unit vector field is defined as $\mathbf{t} := \partial_s \mathbf{\Gamma}$. A local coordinate system can thus be introduced as $\{\mathbf{t}, \mathbf{t}_\perp, \mathbf{k}\}$, where $\mathbf{k} := \mathbf{t} \times \mathbf{t}_\perp$ is a uniform unit vector field and $\mathbf{t}_\perp := \mathbf{R}\mathbf{t}$ is the transversal unit vector field obtained by means of the orthogonal tensor $\mathbf{R}$ (performing the rotation with $\pi/2$ counterclockwise in the plane). According to the linearised Timoshenko beam theory, the tangent deformation field is given by $\{\varepsilon, \gamma, \chi\} : [0, L] \mapsto \Re$, which are the axial strain, shear strain and flexural curvature scalar fields, respectively. The kinematic compatibility condition requires that $\{\varepsilon = \partial_s \mathbf{v} \cdot \mathbf{t}, \gamma = \partial_s \mathbf{v} \cdot \mathbf{t}_\perp - \varphi, \chi = \partial_s \varphi\}$ where $\mathbf{v}$ is the displacement field of the beam axis and φ is the rotation field of the cross-sections. By duality, the stress is given by $\{N, T, M\} : [0, L] \mapsto \Re$ (i.e., the axial force, shear force and bending moment scalar fields, respectively), satisfying the following differential equations of equilibrium:

$$\begin{cases} \partial_s N - T\, \mathbf{t}_\perp \cdot \partial_s \mathbf{t} = -\mathbf{p} \cdot \mathbf{t}\,, \\ \partial_s T - N\, \mathbf{t} \cdot \partial_s \mathbf{t}_\perp = -\mathbf{p} \cdot \mathbf{t}_\perp\,, \\ T + \partial_s M = -\mathrm{m}\,, \end{cases} \tag{43}$$

which are equipped with the boundary conditions at $\partial\mathbf{\Gamma}$:

$$\begin{cases} -(N\mathbf{t} + T\mathbf{t}_\perp)(0) \cdot \delta\mathbf{v}(0) = \mathbf{F}_0 \cdot \delta\mathbf{v}(0)\,, \\ (N\mathbf{t} + T\mathbf{t}_\perp)(L) \cdot \delta\mathbf{v}(L) = \mathbf{F}_L \cdot \delta\mathbf{v}(L)\,, \\ -M(0)\ \delta\varphi(0) = \mathcal{M}_0\ \delta\varphi(0)\,, \\ M(L)\ \delta\varphi(L) = \mathcal{M}_L\ \delta\varphi(L)\,, \end{cases} \tag{44}$$

where $\{\delta\mathbf{v}, \delta\varphi\}$ represents any virtual displacement and rotation field fulfilling the homogeneous kinematic boundary conditions. The external force system in Equations (43) and (44) is made of distributed vector loading $\mathbf{p} : [0, L] \to V$ and bending couples $\mathrm{m} : [0, L] \to \Re$, boundary concentrated forces $\mathbf{F}_0 \in V$ and $\mathbf{F}_L \in V$ and bending couples $\mathcal{M}_0 \in \Re$ and $\mathcal{M}_L \in \Re$.

The stress-driven mixture elasticity can be formulated by introducing the vectors $\mathbf{i}$ and $\mathbf{f}$ collecting the source and output fields, respectively (i.e., $\mathbf{i} = \{\varepsilon_l^{el}, \chi_l^{el}, \gamma_l^{el}\}$; $\mathbf{f} = \{\varepsilon^{el}, \chi^{el}, \gamma^{el}\}$), where the source fields are the local elastic strains, given as

$$\begin{cases} \varepsilon_l^{el}(s) = \dfrac{1}{EA}\left[N + \dfrac{M}{r\,\mathbf{n} \cdot \mathbf{t}_\perp}\right](s)\,, \\ \chi_l^{el}(s) = \dfrac{M}{EJ_r}(s) + (\mathbf{n} \cdot \mathbf{t}_\perp)\dfrac{1}{r\,EA}\left[N + \dfrac{M}{r\,\mathbf{n} \cdot \mathbf{t}_\perp}\right](s)\,, \\ \gamma_l^{el}(s) = \left[\dfrac{T}{GK_r}\right](s)\,, \end{cases} \tag{45}$$

where $\mathbf{n}$ is the normal unit vector, $r^{-1} := |\partial_s \mathbf{t}|$ is the scalar geometric curvature of the beam axis and J_r is the inertia moment along the bending axis η identified by the transversal unit vector $\mathbf{t}_\perp$ (i.e., $J_r = \displaystyle\int_\Omega \eta^2 \frac{r}{r - \eta\,(\mathbf{n} \cdot \mathbf{t}_\perp)}\, dA$), while K_r is the shear stiffness for curved beams, defined in [33]. It is worth noting that in Equation (45), vanishing distributed bending couples have been assumed. Thus, the stress-driven two-phase elastic law is written as follows:

$$\mathbf{f}(s) = \alpha\, \mathbf{i}(s) + (1 - \alpha) \int_0^L \phi_\lambda(s - \xi)\, \mathbf{i}(\xi)\, d\xi\,. \tag{46}$$

The mixture equivalence property extended to Timoshenko curved beams provides the following equivalent differential equation:

$$\frac{\mathbf{f}(s)}{c^2} - \partial_s^2 \mathbf{f}(s) = \frac{\mathbf{i}(s)}{c^2} - \alpha\, \partial_s^2 \mathbf{i}(s) \tag{47}$$

equipped with the constitutive boundary conditions

$$\begin{cases} \partial_s \mathbf{f}(0) = \dfrac{1}{c}\, \mathbf{f}(0) + \alpha \left(\partial_s \mathbf{i}(0) - \dfrac{\mathbf{i}(0)}{c} \right), \\ \partial_s \mathbf{f}(L) = -\dfrac{1}{c}\, \mathbf{f}(L) + \alpha \left(\partial_s \mathbf{i}(L) + \dfrac{\mathbf{i}(L)}{c} \right). \end{cases} \tag{48}$$

Structural problems based on the two-phase elasticity are addressed below with reference to a silicon carbide circular nanobeam of radius $r = 20\,[nm]$. Tables 1 and 2 show the numerical results of the transverse displacements $v_{t_\perp} := \mathbf{v} \cdot \mathbf{t}_\perp$, axial displacements $v_t := \mathbf{v} \cdot \mathbf{t}$ and bending rotations φ of the following structural schemes: cantilever nanobeam under concentrated force $F = 5\,[nN]$ at the free end and slider- and roller-supported nanobeam under uniformly distributed vertical loading $q = 2\,[nN/nm]$ (along the horizontal direction) and directed upward.

Table 1. Cantilever thick nanobeam: numerical outcomes.

λ	$v_\perp(L)$ $[10^{-2}nm]$		$v_t(L)$ $[10^{-2}nm]$		$\varphi(L)$ $[10^{-3}]$		$v^{tot}_{max}(L)$ $[10^{-2}nm]$	
	$\alpha = 0.2$	$\alpha = 0.5$	$\alpha = 0.2$	$\alpha = 0.5$	$\alpha = 0.2$	$\alpha = 0.5$	$\alpha = 0.2$	$\alpha = 0.5$
0.1	2.039	2.118	−1.300	−1.349	0.9429	0.9699	2.418	2.511
0.2	1.818	1.980	−1.170	−1.268	0.8629	0.9199	2.162	2.351
0.3	1.629	1.862	−1.058	−1.198	0.7876	0.8728	1.943	2.214
0.4	1.478	1.768	−0.9655	−1.140	0.7227	0.8323	1.766	2.104
0.5	1.358	1.692	−0.8905	−1.094	0.6686	0.7985	1.624	2.015
0.6	1.261	1.632	−0.8293	−1.055	0.6235	0.7703	1.510	1.944
0.7	1.183	1.583	−0.7787	−1.024	0.5858	0.7468	1.416	1.885
0.8	1.117	1.542	−0.7364	−0.9973	0.554	0.7269	1.338	1.836
0.9	1.062	1.508	−0.7006	−0.9749	0.5269	0.7099	1.273	1.795

Table 2. Slider- and roller-supported thick nanobeam: numerical outcomes.

λ	$v_\perp(0)$ $[10^{-2}nm]$		$v_\perp(L)$ $[10^{-2}nm]$		$\varphi(L)$ $[10^{-3}]$		$v^{tot}_{max}(0)$ $[10^{-2}nm]$	
	$\alpha = 0.2$	$\alpha = 0.5$	$\alpha = 0.2$	$\alpha = 0.5$	$\alpha = 0.2$	$\alpha = 0.5$	$\alpha = 0.2$	$\alpha = 0.5$
0.1	7.233	7.522	−6.970	−7.221	−3.903	−4.03	7.233	7.522
0.2	6.447	7.031	−6.214	−6.748	−3.568	−3.821	6.447	7.031
0.3	5.783	6.616	−5.563	−6.341	−3.261	−3.629	5.783	6.616
0.4	5.252	6.284	−5.042	−6.016	−2.996	−3.464	5.252	6.284
0.5	4.830	6.020	−4.628	−5.757	−2.775	−3.325	4.830	6.020
0.6	4.489	5.807	−4.296	−5.550	−2.591	−3.210	4.489	5.807
0.7	4.211	5.633	−4.026	−5.380	−2.436	−3.113	4.211	5.633
0.8	3.980	5.489	−3.802	−5.241	−2.305	−3.032	3.980	5.489
0.9	3.786	5.367	−3.614	−5.123	−2.193	−2.962	3.786	5.367

The numerical results show a stiffening mechanical behavior for increasing nonlocal parameter λ and a softening response for increasing mixture parameter α. Such a methodology provides a generalization of the stress-driven two-phase theory to the framework of curved stubby beams. Being based on two parameters, the mixture model can be effectively exploited for the modeling and design of small-scale devices based on curved beams.

6.2. Two-Phase Elasticity for Plates

Modeling of two-dimensional nonlocal continua is a topic of current interest in the scientific literature, with a wide range of applications concerning smart ultra-small devices. A stress-driven nonlocal methodology is conceived in [56] to capture scale effects in nanoplates and then generalized in [35] on the basis of a two-phase elasticity theory. The nonlocal mechanics of two-dimensional continua is studied in [31], vibration and buckling analysis of composite nanoplates are carried out in [95], static and dynamic behaviors of nonlocal elastic plates are examined in [96], modeling of circular nanoplate actuators is addressed in [97], chemical sensing systems are proposed in [98], vibration of resonant nanoplate mass sensors is analyzed in [99], nonlinear dynamics of nanoplates is investigated in [100], magneto-electromechanical nanosensors are modeled in [101], thermoelastic damping models for rectangular micro- and nanoplate resonators are proposed in [102], free vibration of functionally graded porous nanoplates is addressed in [103], nonlinear mechanical behavior of porous sandwich nanoplates is characterized in [104], and dynamics of nanoplates is investigated in [99,105].

Stress-driven two-phase elasticity has been recently applied in [35] to capture size-dependent behaviors of two-dimensional continua modeled by the Kirchhoff plate theory. Notably, with reference to an axisymmetric annular plate of internal radius R_i and external radius R_e, a polar coordinate system r, θ, z is conveniently introduced. Moreover, in the following, ∇ will denote the gradient operator and $\otimes$ the tensor product. According to the linearized Kirchhoff theory, the flexural curvature tensor is $\boldsymbol{\chi} := \nabla\nabla u$, denoted by $u : [R_i, R_e] \to \Re$ the transverse displacement field. The kinematic compatibility condition can be explicitly written as $\boldsymbol{\chi} = \partial_r^2 u\, \mathbf{e}_r \otimes \mathbf{e}_r + \dfrac{\partial_r u}{r}\, \mathbf{e}_\theta \otimes \mathbf{e}_\theta$, where the eigenvalues $\partial_r^2 u$ and $\dfrac{\partial_r u}{r}$ are the radial χ_r and circumferential χ_θ curvatures, respectively. The equilibrated stress is given by the radial M_r and circumferential M_θ bending interaction fields, satisfying the following differential equation:

$$\frac{1}{r}\Big(\partial_r^2\big(M_r(r)\cdot r\big) - \partial_r M_\theta(r)\Big) = q(r)\,, \quad r \in \Omega\,, \tag{49}$$

equipped with the boundary condition

$$\begin{cases} M_r(r)\,\partial_r\delta u(r) = -\bar{M}_i\,\partial_r\delta u(r)\,, & r \in \partial\Omega_i \\ M_r(r)\,\partial_r\delta u(r) = \bar{M}_e\,\partial_r\delta u(r)\,, & r \in \partial\Omega_e \\ \Big(M_\theta(r) - \partial_r(M_r(r)\cdot r)\Big)\,\delta u(r) = -\bar{Q}_i\, r\,\delta u(r)\,, & r \in \partial\Omega_i \\ \Big(M_\theta(r) - \partial_r(M_r(r)\cdot r)\Big)\,\delta u(r) = \bar{Q}_e\, r\,\delta u(r)\,, & r \in \partial\Omega_e \end{cases} \tag{50}$$

with q transverse distributed loading, $\{\bar{M}_i, \bar{M}_e\}$ edge distributed bending couples and $\{\bar{Q}_i, \bar{Q}_e\}$ edge distributed transverse forces.

The mixture model of elasticity expresses the elastic radial curvature χ_r^{el} as

$$\chi_r^{el}(r) = \alpha\,\frac{M_r(r) - \nu M_\theta(r)}{D\,(1-\nu^2)} + (1-\alpha)\int_{R_i}^{R_e}\phi_\lambda(r-\xi)\,\frac{M_r(\xi) - \nu M_\theta(\xi)}{D\,(1-\nu^2)}\,d\xi \tag{51}$$

where ν is Poisson's ratio and D is the plate flexural stiffness.

In Equation (51), $\lambda := \dfrac{c}{(R_e - R_i)}$ is the nonlocal parameter, while α is the mixture parameter providing the purely nonlocal and local responses for $\alpha = 0$ and $\alpha = 1$, respectively. By adopting the bi-exponential special kernel, an equivalent differential formulation can be provided. Specifically, the convex combination in Equation (51) is equivalent to the following differential equation:

$$\frac{\chi_r^{el}(r)}{c^2} - \partial_r^2 \chi_r^{el}(r) = \frac{M_r(r) - \nu M_\theta(r)}{c^2\, D\,(1-\nu^2)} - \alpha\, \frac{\partial_r^2 (M_r(r) - \nu M_\theta(r))}{D\,(1-\nu^2)}, \tag{52}$$

equipped with the constitutive boundary conditions

$$\begin{cases} \partial_r \chi_r^{el}(r)\Big|_{r=R_i} - \dfrac{1}{c}\,\chi_r^{el}(R_i) = \alpha \left(\dfrac{\partial_r (M_r(r) - \nu M_\theta(r))}{D\,(1-\nu^2)} - \dfrac{M_r(r) - \nu M_\theta(r)}{c\, D\,(1-\nu^2)} \right)\Big|_{r=R_i}, \\ \partial_r \chi_r^{el}(r)\Big|_{r=R_e} + \dfrac{1}{c}\,\chi_r^{el}(R_e) = \alpha \left(\dfrac{\partial_r (M_r(r) - \nu M_\theta(r))}{D\,(1-\nu^2)} + \dfrac{M_r(r) - \nu M_\theta(r)}{c\, D\,(1-\nu^2)} \right)\Big|_{r=R_e}. \end{cases} \tag{53}$$

The mixture elasticity is adopted to solve the structural problem of a graphene nanoplate with a Euler–Young modulus $E = 1\,[TPa]$ and Poisson's ratio $\nu = 0.25$ and external and internal radii $R_e = 30\,[nm]$ and $R_i = 3\,[nm]$, respectively. The nanoplate has clamped edges and is subjected to a uniformly distributed transverse loading $q = -10^{-3}\,[nN/nm^2]$. Parametric studies are carried out to simulate size effects and as depicted in Figure 8, a stiffening effect is obtained for increasing λ values for a fixed mixture parameter. Since it is based on two parameters, the stress-driven two-phase elasticity is able to simulate a wide class of nanotechnological applications involving miniaturized devices based on nanoplates.

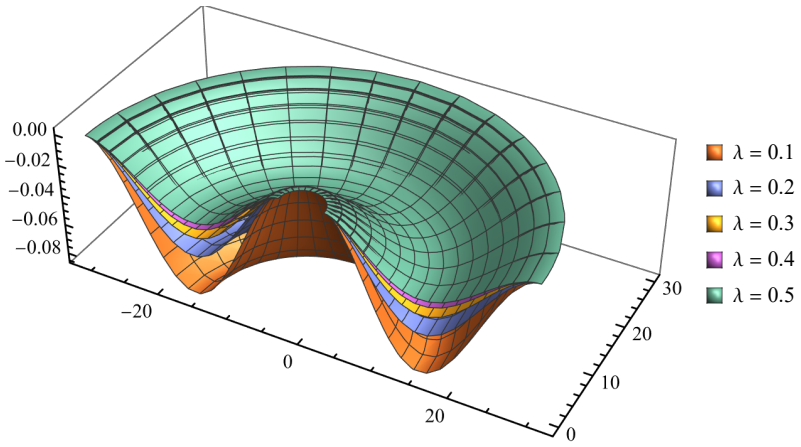

Figure 8. Nanoplate with clamped edges under uniformly distributed loading: transverse displacement fields $u\,[nm]$ for $\alpha = 0.2$.

7. Dynamics of Nanobeams

The dynamic problem of a slender nanobeam is formulated by exploiting the general two-phase local/nonlocal methodology. The beam is assumed to lay on a bed of dashpots with a viscosity η, providing a damping effect. The differential equation of the d'Alembert dynamic equilibrium for a slender beam is $\partial_x^2 M = q - \eta\,\dot{v} - m\,\ddot{v}$ where q is a transverse distributed loading and m denotes the mass per unit length. The symbol dot will be applied in the following to denote the time derivative. According to the stress-driven mixture theory of elasticity applied to slender beams, the nonlocal response $f := \chi^{el}$ is convex combination of the local source field $s := k_f^{-1}\, M$ and the purely stress-driven convolution integral $\phi_\lambda * s$.

By adopting the equivalent differential formulation and differentiating twice, the following equation is found:

$$\frac{1}{c^2}\,\partial_x^2\chi^{el}(x,\,t)-\partial_x^4\chi^{el}(x,\,t)=\frac{1}{c^2}\,\frac{\partial_x^2 M(x,\,t)}{k_f}-\alpha\frac{\partial_x^4 M(x,\,t)}{k_f}\,, \tag{54}$$

which can be further manipulated by prescribing the compatibility condition and the equilibrium requirements in order to find the differential equation governing the bending vibrations:

$$\frac{1}{c^2}\,\partial_x^4 v(x,\,t)-\partial_x^6 v(x,\,t)=-\frac{1}{c^2}\,\frac{m\ddot{v}(x,\,t)}{k_f}+\alpha\,m\frac{\partial_x^2\ddot{v}(x,\,t)}{k_f}\,. \tag{55}$$

With the aim of first investigating the free vibration problem of an undamped beam, vanishing loading and viscosity have been assumed in deriving Equation (55). Moreover, synchronous motions $v(x,t)$ will be investigated, which are mathematically represented by the assumption that the solution $v(x,t)$ to Equation (55) is separable in spatial and time variables (i.e., $v(x,t)=\psi(x)\,y(t)$). The following differential equations can thus be provided:

$$\begin{cases}\ddot{y}(t)+\omega^2\,y(t)=0\,,\\ \partial_x^6\psi(x)-\dfrac{1}{c^2}\partial_x^4\psi(x)+\dfrac{m\,\omega^2\,\psi(x)}{c^2\,k_f}=0\,,\end{cases} \tag{56}$$

where $\alpha=0$ is assumed. The first in Equation (56) is the differential equation governing harmonic motion, whose evaluation requires prescription of suitable initial conditions. The second in Equation (56) is a sixth-order differential equation in the unknown ψ that must be equipped with four standard boundary conditions and the following two constitutive boundary conditions:

$$\begin{cases}\partial_x^3\psi(0)-\dfrac{1}{c}\,\partial_x^2\psi(0)=0\,,\\ \partial_x^3\psi(L)+\dfrac{1}{c}\,\partial_x^2\psi(L)=0\,.\end{cases} \tag{57}$$

providing the differential problem of eigenvalues ω and eigenfunctions $\phi(x)$ which admits infinite solutions. Now, let us analyze the forced vibration problem of a damped beam governed by the following equation:

$$\frac{1}{c^2}\,\partial_x^4 v(x,\,t)-\partial_x^6 v(x,\,t)+\frac{1}{c^2}\,\frac{\eta\dot{v}(x,\,t)}{k_f}+\frac{1}{c^2}\,\frac{m\ddot{v}(x,\,t)}{k_f}=\frac{1}{c^2}\,\frac{q(x,\,t)}{k_f}\,. \tag{58}$$

The solution $v(x,t)=\sum_{j=1}^{\infty}\psi_j(z)y_j(t)$ can be inserted into Equation (58). Then, multiplying both sides by the ith eigenfunction ψ_i and integrating over the domain yield

$$\ddot{y}_i(t)+\frac{\eta}{m}\dot{y}_i(t)+\frac{k_{\lambda,i}}{m}\,y_i(t)=\frac{\int_0^L\psi_i(x)\,q(x,t)\,dx}{m}\,, \tag{59}$$

where the orthonormality property of the eigenfunctions has been taken into account. The symbol $k_{\lambda,i}$ in Equation (59) denotes the nonlocal stiffness defined in [106].

Random vibrations are now analyzed to take into account the stochastic nature of the external loadings and simulate the conditions of micro- and nanodevices subjected to environmental noise. Notably, the loading is assumed to be $q(x,t):=g(x)\,F(t)$ where g is a deterministic function and F is a stochastic process. Specifically, F is assumed to be a stationary Gaussian process with a zero mean $\mu_F:=\mathbb{E}[F(t)]$ and correlation function $R_F(\tau):=\mathbb{E}[F(t)F(t+\tau)]$. A frequency domain approach can be followed to

characterize the steady state response of the output process in terms of beam displacements. The differential Equation (59) is written as

$$\ddot{Y}_i(t) + \frac{\eta}{m}\dot{Y}_i(t) + \frac{k_{\lambda,i}}{m}Y_i(t) = \frac{a_i}{m}F(t)\,, \tag{60}$$

where $a_i := \int_0^L \psi_i(x)\, g(x) dx$. The truncated Fourier transform of Equation (60) is then performed to find the response in the frequency domain:

$$\hat{Y}_i(\omega, \mathrm{T}) = \frac{1}{-\omega^2 + \frac{\eta}{m}\mathrm{i}\omega + \frac{k_{\lambda,i}}{m}} \frac{a_i}{m}\hat{F}(\omega, \mathrm{T})\,, \tag{61}$$

where the symbol $\hat{}$ stands for the truncated Fourier transform in the time interval $[0,\ T]$ and i is the imaginary unit. By exploiting Equation (61), the analytical form of the power spectral density function can be derived:

$$S_v(x,\omega) = \sum_{j=1}^{\infty}\sum_{i=1}^{\infty} \psi_j(x)\psi_i(x) \lim_{\mathrm{T}\to\infty} \frac{1}{2\pi\mathrm{T}} \mathbb{E}\left[\hat{Y}_j^*(\omega, \mathrm{T})\hat{Y}_i(\omega, \mathrm{T})\right], \tag{62}$$

where the apex $*$ denotes the complex conjugate. Finally, the stationary variance of the beam displacements is computed by integration of the power spectral density function over the frequency domain $\sigma_v^2(x) = \int_{-\infty}^{\infty} S_v(x,\omega)\, d\omega$.

The free vibration response is investigated with reference to a slender, nonlocal elastic cantilever of a unit length. Figure 9 represents the first five nonlocal eigenfunctions for a nonlocal parameter $\lambda = 0.15$, obtained by solving Equation $(56)_2$ equipped with the standard boundary conditions and with the constitutive boundary conditions in Equation (57).

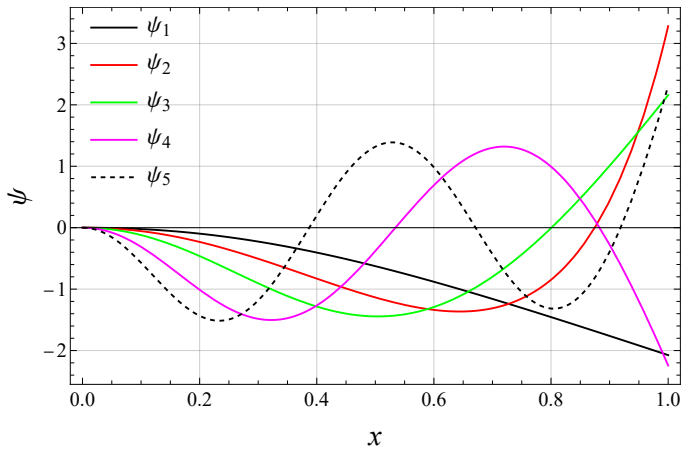

Figure 9. First five eigenfunctions of nonlocal elastic cantilever for nonlocal parameter $\lambda = 0.15$.

Random vibrations of small-scale beams are investigated in [106], where both frequency and time domain responses are evaluated. Notably, the non-stationary variance of displacements is provided by performing a Monte Carlo simulation, assuming that the beam is loaded by a stationary Gaussian process. A proper number of realizations of the stochastic input process is generated by the formula proposed by Shinozuka and Deodatis in [107]. The output process is then obtained by applying the Duhamel superposition integral, and finally the displacement samples are processed to evaluate the non-stationary variance. Further contributions exploring dynamics of nonlocal continua are provided in [108], where nanobeam-based resonators are investigated, in [109], concerning forced vibrations of dielectric elastomer-based microcantilevers, in [110], where buckling of graphene platelet-reinforced nanostructures is examined, in [111], which concerns dynam-

ics of a piezoelectric semiconductor nanoplate, in [112], in which dynamics of nonlocal rods is examined, in [113], where transverse vibrations of nanobeams with multiple cracks are evaluated, and in [114], in which mechanical static and dynamic behaviors of microsystems are investigated providing fundamental concepts of modeling and design.

Transient response of functionally graded nanobeams is investigated in [115], buckling problem of nonhomogeneous microbeams is addressed in [116], linear and nonlinear dynamic responses of microsystems are evaluated in [117], thermo-mechanical vibration analysis of nanobeams is performed in [118], free vibration of embedded carbon and silica carbide nanotubes is analyzed in [119], dynamic analysis of nanostructures exploiting the Chebyshev–Ritz method is provided in [120], and nonlinear dynamics of nanobeams connected with fullerenes is investigated in [121].

8. Nonlocal Elasticity for Structural Assemblages

In this section, a nonlocal methodology is illustrated to account for size effects in structural assemblages. Notably, convolution integrals involving piecewise regular source fields are investigated to model beam problems involving discontinuous and concentrated loadings, non-smooth elastic and geometric properties and internal kinematic constraints, which are the most general cases when dealing with structural problems. In this context, the stress-driven integral theory of elasticity has been recently developed to capture size effects in assemblages of slender beams [122]. For this purpose, the next proposition plays a fundamental role in the development of nonlocal strategies for complex structural systems:

Proposition 3. *The nonlocal elastic curvature obtained with Equation* (27) *is a continuously differentiable field* $\chi^{el} \in \mathrm{C}^1([0,L];\Re)$ *for any piecewise smooth local source field.*

Let us suppose that we have a beam partitioned into two domains of regularity. The integral constitutive law in Equation (27), equipped with the special kernel, can be explicitly written as

$$\chi^{el}(x) = \begin{cases} \dfrac{1}{2c}\displaystyle\int_0^x exp\left(\frac{\xi - x}{c}\right)\frac{M_1}{I_{E1}}(\xi)d\xi + \frac{1}{2c}\int_x^{x_d} exp\left(\frac{x-\xi}{c}\right)\frac{M_1}{I_{E1}}(\xi)d\xi \\ + \dfrac{1}{2c}\displaystyle\int_{x_d}^L exp\left(\frac{x-\xi}{c}\right)\frac{M_2}{I_{E2}}(\xi)d\xi, \qquad x \in [0, x_d], \\ \dfrac{1}{2c}\displaystyle\int_0^{x_d} exp\left(\frac{\xi - x}{c}\right)\frac{M_1}{I_{E1}}(\xi)d\xi + \frac{1}{2c}\int_{x_d}^x exp\left(\frac{\xi-x}{c}\right)\frac{M_2}{I_{E2}}(\xi)d\xi \\ + \dfrac{1}{2c}\displaystyle\int_x^L exp\left(\frac{x-\xi}{c}\right)\frac{M_2}{I_{E2}}(\xi)d\xi, \qquad x \in [x_d, L], \end{cases} \tag{63}$$

with $M_1 : [0, x_d] \mapsto \Re$ and $M_2 : [x_d, L] \mapsto \Re$ regular bending interaction fields and $I_{E1} : [0, x_d] \mapsto \Re$ and , $I_{E2} : [x_d, L] \mapsto \Re$ regular bending stiffnesses, which represents the second moment of the Euler–Young modulus field on the beam cross-sections. It can be immediately proven that the nonlocal curvature generated by the convolution integral in Equation (63) is a continuously differentiable field in $[0, L]$. Indeed, its first derivative is given by

$$\partial_x \chi^{el}(x) = \begin{cases} \frac{1}{2c^2}\left(-\int_0^x exp\left(\frac{\xi - x}{c}\right)\frac{M_1}{I_{E1}}(\xi)d\xi + \int_x^{x_d} exp\left(\frac{x-\xi}{c}\right)\frac{M_1}{I_{E1}}(\xi)d\xi \right. \\ \left. + \int_{x_d}^{L} exp\left(\frac{x-\xi}{c}\right)\frac{M_2}{I_{E2}}(\xi)d\xi\right), \qquad x \in [0, x_d]\,, \\ \frac{1}{2c^2}\left(-\int_0^{x_d} exp\left(\frac{\xi - x}{c}\right)\frac{M_1}{I_{E1}}(\xi)d\xi - \int_{x_d}^{x} exp\left(\frac{\xi-x}{c}\right)\frac{M_2}{I_{E2}}(\xi)d\xi \right. \\ \left. + \int_{x}^{L} exp\left(\frac{x-\xi}{c}\right)\frac{M_2}{I_{E2}}(\xi)d\xi\right), \qquad x \in [x_d, L]\,, \end{cases} \tag{64}$$

which is a continuous field in $[0, L]$. Proposition 3 plays a key role in proving the equivalent constitutive differential formulation. Indeed, the constitutive differential problem is made of the following set of differential equations, each one referring to a subdomain of regularity:

$$\begin{cases} \frac{1}{c^2}\chi_1^{el}(x) - \partial_x^2\chi_1^{el}(x) = \frac{1}{c^2}\frac{M_1}{I_{E1}}(x)\,, \qquad x \in [0, x_d]\,, \\ \frac{1}{c^2}\chi_2^{el}(x) - \partial_x^2\chi_2^{el}(x) = \frac{1}{c^2}\frac{M_2}{I_{E2}}(x)\,, \qquad x \in [x_d, L]\,, \end{cases} \tag{65}$$

equipped with constitutive boundary condition at $\partial[0, L]$

$$\begin{cases} \partial_x\chi_1^{el}(0) = \frac{1}{c}\chi_1^{el}(0)\,, \\ \partial_x\chi_2^{el}(L) = -\frac{1}{c}\chi_2^{el}(L)\,, \end{cases} \tag{66}$$

and interface boundary conditions at the internal abscissa x_d:

$$\begin{cases} \chi_1^{el}(x_d) = \chi_2^{el}(x_d)\,, \\ \partial_x\chi_1^{el}(x_d) = \partial_x\chi_2^{el}(x_d)\,. \end{cases} \tag{67}$$

The interface continuity conditions in Equation (67) can be prescribed by virtue of Proposition 3. These constitutive interface conditions play a fundamental role in modeling the assemblages of nonlocal elastic structures, and it is worth noting that they do not involve any convolution integrals and thus can be conveniently adopted for formulating and solving the structural problems of complex nanosystems. The constitutive conditions in Equation (67) are equivalent to those established in [123], which involve convolution integrals.

The theoretical outcomes illustrated in this Section are confirmed in the sequel by investigating a structural scheme involving a piecewise regular local field of elastic curvature induced by a concentrated loading. For this purpose, a nonlocal elastic beam with clamped and simply supported ends under a concentrated couple $\mathcal{M}$ at mid-span is analyzed, and the parametric responses will be provided for increasing the length scale parameter $\lambda = c/L$. Figure 10 shows the solutions in terms of the non-dimensional elastic curvature $\bar{\chi}^{el}(\bar{x}) = \chi^{el}(x)\frac{I_E}{\mathcal{M}}$ versus the non-dimensional abscissa $\bar{x} = x/L \in [0, 1]$. As theoretically predicted, the nonlocal fields $\bar{\chi}^{el}$ are continuously differentiable functions for $\lambda > 0$ and become more uniform as λ increases. It is interesting to analyze the asymptotic behavior for $\lambda \to 0^+$, showing that the local elastic curvature is recovered for $\bar{x} \in]0, 1] - \{\bar{x}_d\}$. At the external boundary abscissa $\bar{x} = 0$, one half of the local elastic curvature is got, and at the interior point $\bar{x} = 1/2$, the limiting response is equal to the average of the local elastic curvatures. These peculiar behaviors are due to the asymptotic behavior of the

kernel. The non-dimensional fields of the transverse displacements $\bar{v}(\bar{x}) = v(x)\dfrac{I_E}{\mathcal{M}L^2}$ are shown in Figure 11. It is worth noting that the limiting solution is coincident with the local displacement, since the asymptotic peculiar behaviors only affect the null measure sets. The presented differential formulation, involving the prescription of constitutive boundary and interface conditions, plays a key role in conceiving a finite-element nonlocal methodology, as shown in [124]. Further contributions to this topic can be found in [125], where nanobeams with internal discontinuities are investigated by exploiting a mixture approach, and in [126], where strain- and stress-driven differential formulations of Timoshenko nanobeams with loading discontinuities are provided.

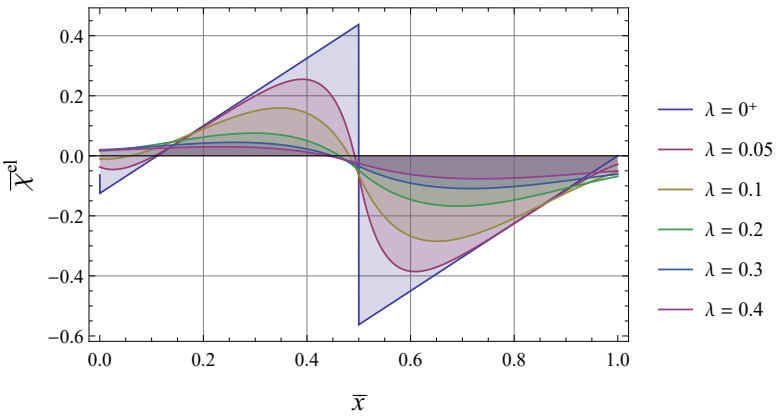

Figure 10. Beam with clamped and simply supported ends under concentrated couple $\mathcal{M}$ at mid-span $\bar{x} = 1/2$: elastic curvature $\bar{\chi}^{el}$ versus $\bar{x}$ for increasing nonlocal parameter λ.

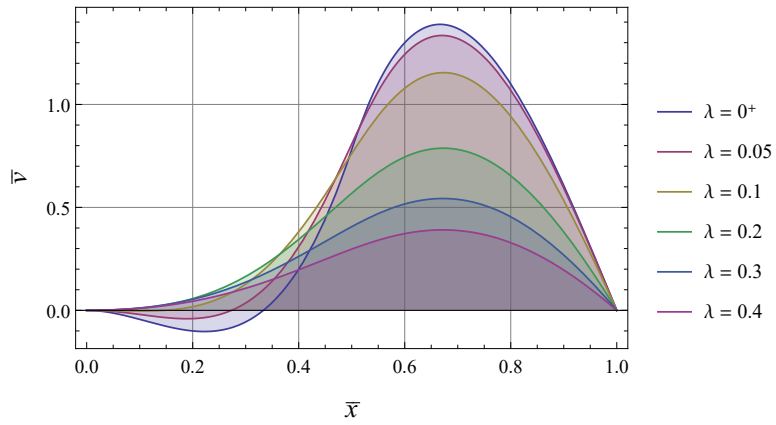

Figure 11. Beam with clamped and simply supported ends under concentrated couple $\mathcal{M}$ at mid-span $\bar{x} = 1/2$: transverse displacement $\bar{v} \cdot 10^{-2}$ versus $\bar{x}$ for increasing nonlocal parameter λ.

9. Nanostructures on Nonlocal Foundations

Many contributions in the scientific literature deal with the modeling of nanobeams resting on elastic soils, since they are involved in several biomechanical and biomedical applications of current interest. Dynamics of nanobeams on Pasternak soil is addressed in [127,128]. Buckling of small-scale structures embedded in two parameter foundations is investigated in [129,130]. Elastostatics of nanostructures on Winkler soil is examined in [131]. Free vibration of nanobeams on Pasternak soil is addressed in [132]. Nanobeams embedded in cell cytoplasm are analyzed in [133]. Nonlinear vibration analysis of nanobeams interacting with an elastic medium is carried out in [134]. The interaction between nanoshells and elastic foundations is studied in [135]. Magnetically embedded composite nanobeams are analyzed in [136]. Stability of nonlocal beams exposed to a hygro-thermo-magnetic environment and lying on elastic foundations is addressed in [137].

Vibration of functionally graded beams on a viscoelastic Winkler–Pasternak foundation is investigated in [90]. Buckling of Bernoulli–Euler nanobeams resting on a Pasternak elastic foundation is examined in [138]. Recent achievements regarding this topic are provided in [139], where mechanics of nanobeams on nano-foundations is addressed on the basis of the nonlocal model of elastic medium proposed in [140].

In order to assure that the relevant structural foundation problem is well-posed, it is necessary that the integral constitutive laws of internal and external elasticity are compatible with both the equilibrium and compatibility requirements. In the framework of nonlocal internal elasticity, the strain-driven purely integral approach proved itself to be incompatible with the equilibrium requirements, and as shown in Section 2, the equivalence property provided an effective tool to check the consistency. Indeed, according to Proposition 2, the constitutive integral law in Equation (12) admits a unique solution if and only if the equilibrated bending interaction field satisfies the constitutive boundary conditions in Equation (13). These constitutive boundary conditions are, in general, in contrast with the natural ones, and thus no solution exists to Equation (12), since the integral constitutive law is incompatible with the equilibrium requirements. In Section 4, a new integral model is shown, the stress-driven theory, which is able to overcome the intrinsic issues emerged from the strain-driven approach. Thus, source fields in the convolution integral play a fundamental role in providing a consistent constitutive theory. In the context of external integral elasticity, the Wieghardt model [141] provides a refinement of the Winkler local theory of elastic foundation by assuming that the beam deflection v is a convolution integral between a proper averaging kernel ϕ and the soil reaction field r. Concerning the Wieghardt theory, also referred to as the reaction-driven model, the following equivalence property can be stated:

Proposition 4. *For any characteristic length $c_f > 0$, the integral constitutive law*

$$v(x) = \int_0^L \phi(x-\xi, c_f)\, \frac{r(\xi)}{k} d\xi \tag{68}$$

equipped with the bi-exponential kernel in Equation (4) admits either a unique solution or no solution at all, depending on whether or not the interface displacement field satisfies the following constitutive boundary conditions:

$$\begin{cases} \partial_x v(0) = \dfrac{1}{c_f} v(0)\,, \\ \partial_x v(L) = -\dfrac{1}{c_f} v(L)\,. \end{cases} \tag{69}$$

If Equation (69) is fulfilled by the compatible displacement field, then the unique solution v is obtained from the second-order differential equation

$$v(x) - c_f^2\, \partial_x^2 v(x) = \frac{r(x)}{k}\,, \tag{70}$$

where k is the Winkler local stiffness of the foundation. It is apparent that an incompatibility arises between the kinematic and constitutive (Equation (69)) boundary conditions, since the latter relates to the displacement and rotation at the beam ends for any value of the characteristic parameter. These requirements are not satisfied by the kinematic boundary conditions generally involved in technical applications. A mathematical trick to overcome this issue was provided in [142], but it requires the introduction of fictitious reactive forces that have no physical meaning. An effective strategy has been then proposed in [140] to overcome the ill-posed nature of the structural problem of beams on a Wieghardt foundation. This new integral theory of foundation is based on a displacement-driven

approach [140] requiring that the foundation reaction is expressed as a convolution integral driven by the interface transverse displacement:

$$r(x) = \int_0^L \phi(x-\xi,\, c_f) k\, v(\xi) d\xi\,. \tag{71}$$

As proven in [140], the constitutive integral law in Equation (71) is a consistent theory providing well-posed structural problems. Such a new model of nonlocal elastic foundation can be effectively exploited to model the size-dependent behavior of nanobeams lying on nano-foundations. Notably, the stress-driven theory of elasticity can be adopted to capture size effects in small-scale beams, while the surrounding medium can be modeled by the displacement-driven nonlocal approach. The relevant structural problem of a small-scale beam of length L and local elastic inertia $k_f := I_E$ laying on a nonlocal elastic foundation with a local stiffness k can thus be expressed as follows:

$$\begin{cases} \partial_x^2 M(x) = q(x) - r(x)\,, \\ r(x) = \displaystyle\int_0^L \phi\Big(x-\xi,\, c_f\Big) k\, v(\xi) dt\,, \\ \chi^{el}(x) = \displaystyle\int_0^L \phi(x-\xi,\, c_b) \frac{M(\xi)}{I_E} d\xi\,, \\ \partial_x^2 v(x) = \chi(x)\,, \end{cases} \tag{72}$$

where c_b is the beam's characteristic length. System in Equation (72) consists of the beam differential equation of equilibrium, the displacement-driven law of external elasticity, the stress-driven law of internal elasticity and the beam kinematic compatibility condition. It is worth noting that non-elastic effects are not taken into account in the following, so $\chi = \chi^{el}$. The structural foundation problem in Equation (72) is equipped with the standard boundary conditions involving $\{v,\, \varphi,\, M,\, T\}$, where $\varphi := \partial_x v$ and $T := -\partial_x M$. By virtue of the equivalence property proven in [139], the integro-differential problem (Equation (72)) can be reverted to a simpler differential formulation:

$$\begin{cases} c_b^2\, c_f^2\, \partial_x^8 r(x) - \Big(c_b^2 + c_f^2\Big)\, \partial_x^6 r(x) + \partial_x^4 r(x) + \dfrac{k}{I_E} r(x) = \dfrac{k}{I_E} q_y(x)\,, \\ \partial_x^3 r(0) - c_f^2\, \partial_x^5 r(0) = \dfrac{1}{c_b}\Big(\partial_x^2 r(0) - c_f^2\, \partial_x^4 r(0)\Big)\,, \\ \partial_x^3 r(L) - c_f^2\, \partial_x^5 r(L) = -\dfrac{1}{c_b}\Big(\partial_x^2 r(L) - c_f^2\, \partial_x^4 r(L)\Big)\,, \\ \partial_x r(0) = \dfrac{1}{c_f} r(0)\,, \\ \partial_x r(L) = -\dfrac{1}{c_f} r(L)\,, \end{cases} \tag{73}$$

equipped with essential and natural boundary conditions involving the following fields:

$$\begin{cases} v(x) = \dfrac{1}{k} r(x) - \dfrac{c_f^2}{k}\, \partial_x^2 r(x)\,, \\ \varphi(x) = \dfrac{1}{k} \partial_x r(x) - \dfrac{c_f^2}{k}\, \partial_x^3 r(x)\,, \\ M(x) = \dfrac{I_E}{k} \partial_x^2 r(x) - \dfrac{I_E}{k} c_f^2\, \partial_x^4 r(x) - \dfrac{I_E}{k} c_b^2\, \partial_x^4 r(x) + \dfrac{I_E}{k} c_b^2\, c_f^2\, \partial_x^6 r(x)\,, \\ T(x) = -\dfrac{I_E}{k} \partial_x^3 r(x) + \dfrac{I_E}{k} c_f^2\, \partial_x^5 r(x) + \dfrac{I_E}{k} c_b^2\, \partial_x^5 r(x) - \dfrac{I_E}{k} c_b^2\, c_f^2\, \partial_x^7 r(x)\,. \end{cases} \tag{74}$$

Effectiveness of the proposed nonlocal methodology is proven by the numerical outcomes of technical interest illustrated in [139]. As a benchmark case study, let us consider a simply supported beam on a nonlocal foundation under non-dimensional transverse loading $q^* := \dfrac{q\,L^3}{I_E} = 1$. Solution of the relevant structural problem in Equation (73) equipped with standard (essential and natural) boundary conditions provides the non-dimensional displacement field $v^* := \dfrac{v}{L}$ represented in Figure 12, for a fixed non-dimensional stiffness $k^* := \dfrac{k\,L^4}{I_E} = 100$, showing a softening behavior for increasing foundation parameter $\lambda_f := \dfrac{c_f}{L}$. Non-dimensional bending interaction fields $M^* := \dfrac{M\,L}{I_E}$ are represented in Figure 13 for increasing values of λ_f.

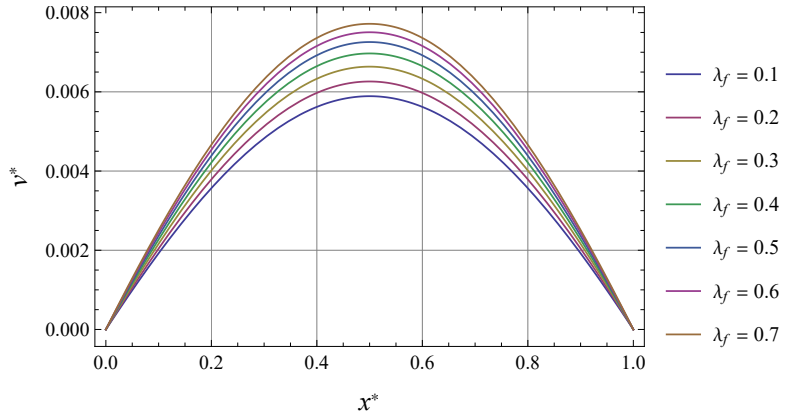

Figure 12. Non-dimensional transverse displacement fields for $k^* = 100$ and $\lambda_b = 0.2$.

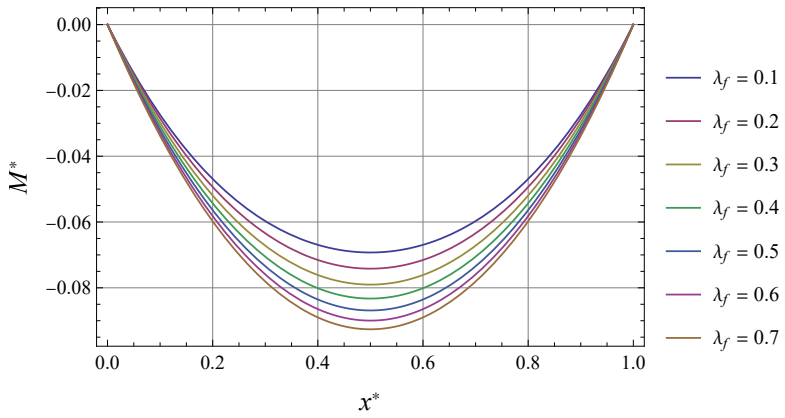

Figure 13. Non-dimensional bending interaction fields for $k^* = 100$ and $\lambda_b = 0.2$.

10. Conclusions

In the paper, recent achievements in the framework of modeling and analysis of nanostructures have been illustrated and critically discussed. A comprehensive overview on nonlocal continuum mechanics has been provided, starting from the early concepts contributed by Eringen. Alternative theories of nonlocal elasticity in the strain-driven formulation have been analyzed and discussed, such as mixture local/Eringen nonlocal model and strain difference-based theories. Stress-driven nonlocal methodologies recently proposed in literature to capture size-dependent static and dynamic behaviors of nanostructures have been collected and examined. In this framework, the stress-driven two-phase (local/nonlocal) model has been shown to be an effective tool to capture a wide class of ultra-small devices. Achievements in the field of integral elasticity applied to geometrically nonlinear mechanics of inflected nanostructures undergoing large configuration changes have been then elucidated and commented upon. A challenging issue in nonlocal mechanics has been then addressed concerning reproducibility of continuum structural problems. Nonlocal methodologies for structural assemblages have been thus inspected according to the stress-driven approach and benchmark case studies have been provided. Recent original contributions regarding mechanics of nanobeams on nonlocal foundations have been finally analyzed to address challenging applications of current interest.

Author Contributions: All the authors contributed equally to this work. All authors have read and agreed to the published version of the manuscript.

Funding: Financial support from the Italian Ministry of Education, University and Research (MIUR) in the framework of the Project PRIN—code 2017J4EAYB, Multiscale Innovative Materials and Structures (MIMS)—and from the research program ReLUIS 2020–2021 are gratefully acknowledged.

Institutional Review Board Statement: Not applicable.

Informed Consent Statement: Not applicable.

Data Availability Statement: The data presented in this study are available within this article. Further inquiries may be directed to the authors.

Conflicts of Interest: The authors declare no conflict of interest.

References

1. Rogula, D. Influence of spatial acoustic dispersion on dynamical properties of dislocations. *Bull. Pol. Acad. Sci. Tech. Sci.* **1965**, *13*, 337–385.
2. Kröner, E. Elasticity theory of materials with long range cohesive forces. *Int. J. Solids Struct.* **1967**, *3*, 731–742. [CrossRef]
3. Meo, M.; Rossi, M. Prediction of Young's modulus of single wall carbon nanotubes by molecular-mechanics based finite element modeling. *Compos. Sci. Technol.* **2006**, *66*, 1597–1605. [CrossRef]
4. Malagù, M.; Benvenuti, E.; Simone, A. One-dimensional nonlocal elasticity for tensile single-walled carbon nanotubes: A molecular structural mechanics characterization. *Eur. J. Mech.—A/Solids* **2015**, *54*, 160–170. [CrossRef]
5. Duan, K.; Li, L.; Hu, Y.; Wang, X. Enhanced interfacial strength of carbon nanotube/copper nanocomposites via Ni-coating: Molecular-dynamics insights. *Phys. E Low-Dimens. Syst. Nanostructures* **2017**, *88*, 259–264. [CrossRef]
6. Eringen, A.C. Linear theory of nonlocal elasticity and dispersion of plane waves. *Int. J. Eng. Sci.* **1972**, *10*, 425–435. [CrossRef]
7. Eringen, A.C. On differential equations of nonlocal elasticity and solutions of screw dislocation and surface waves. *J. Appl. Phys.* **1983**, *54*, 4703–4710. [CrossRef]
8. Romano, G.; Barretta, R. Stress-driven versus strain-driven nonlocal integral model for elastic nano-beams. *Compos. B. Eng.* **2017**, *114*, 184–188. [CrossRef]
9. Peddieson, J.; Buchanan, G.R.; McNitt, R.P. Application of nonlocal continuum models to nanotechnology. *Int. J. Eng. Sci.* **2003**, *41*, 305–312. [CrossRef]
10. Challamel, N.; Wang, C.M. The small length scale effect for a non-local cantilever beam: A paradox solved. *Nanotechnology* **2008**, *19*, 345703. [CrossRef]
11. Romano, G.; Barretta, R.; Diaco, M. On nonlocal integral models for elastic nano-beams. *Int. J. Mech. Sci.* **2017**, *131-132*, 490–499. [CrossRef]
12. Eringen, A.C. Theory of nonlocal elasticity and some applications. *Res. Mech.* **1987**, *21*, 313–342.
13. Eringen, A.C. *Nonlocal Continuum Field Theories*; Springer: New York, NY, USA, 2002.
14. Khodabakhshi, P.; Reddy, J. A unified integro-differential nonlocal model. *Int. J. Eng. Sci.* **2015**, *95*, 60–75. [CrossRef]

15. Pisano, A.A.; Fuschi, P. Closed form solution for a nonlocal elastic bar in tension. *Int. J. Solids Struct.* **2003**, *40*, 13–23. [CrossRef]
16. Fuschi, P.; Pisano, A.; Polizzotto, C. Size effects of small-scale beams in bending addressed with a strain-difference based nonlocal elasticity theory. *Int. J. Mech. Sci.* **2019**, *151*, 661–671. [CrossRef]
17. Aifantis, E.C. Update on a class of gradient theories. *Mech. Mater.* **2003**, *35*, 259–280. [CrossRef]
18. Aifantis, E.C. Exploring the applicability of gradient elasticity to certain micro/nano reliability problems. *Microsyst. Technol.* **2009**, *15*, 109–115. [CrossRef]
19. Aifantis, E.C. On the gradient approach–relation to Eringen's nonlocal theory. *Int. J. Eng. Sci.* **2011**, *49*, 1367–1377. [CrossRef]
20. Lim, C.; Zhang, G.; Reddy, J. A higher-order nonlocal elasticity and strain gradient theory and its Applications in wave propagation. *J. Mech. Phys. Solids* **2015**, *78*, 298–313. [CrossRef]
21. Barretta, R.; Marotti de Sciarra, F. Constitutive boundary conditions for nonlocal strain gradient elastic nano-beams. *Int. J. Eng. Sci.* **2018**, *130*, 187–198. [CrossRef]
22. Barretta, R.; Faghidian, S.; Marotti de Sciarra, F.; Vaccaro, M. Nonlocal strain gradient torsion of elastic beams: Variational formulation and constitutive boundary conditions. *Arch. Appl. Mech.* **2020**, *90*, 691–706. [CrossRef]
23. Gurtin, M.; Murdoch, A. A Continuum Theory of Elastic Material Surfaces. *Arch. Ration. Mech. Anal.* **1975**, *57*, 291–323. [CrossRef]
24. Li, L.; Lin, R.; Ng, T.Y. Contribution of nonlocality to surface elasticity. *Int. J. Eng. Sci.* **2020**, *152*, 103311. [CrossRef]
25. Carbone, L.; Gaudiello, A.; Hernández-Llanos, P. T-junction of ferroelectric wires. *ESAIM Math. Model. Numer. Anal.* **2020**, *54*, 1429–1463. [CrossRef]
26. Gaudiello, A.; Sili, A. Limit models for thin heterogeneous structures with high contrast. *J. Differ. Equ.* **2021**, *302*, 37–63. [CrossRef]
27. Romano, G.; Barretta, R. Nonlocal elasticity in nanobeams: The stress-driven integral model. *Int. J. Eng. Sci.* **2017**, *115*, 14–27. [CrossRef]
28. Barretta, R.; Marotti de Sciarra, F.; Vaccaro, M.S. On nonlocal mechanics of curved elastic beams. *Int. J. Eng. Sci.* **2019**, *144*, 103140. [CrossRef]
29. Romano, G.; Barretta, R.; Diaco, M. Iterative methods for nonlocal elasticity problems. *Contin. Mech. Thermodyn.* **2019**, *31*, 669–689. [CrossRef]
30. Sedighi, H.M.; Malikan, M. Stress-driven nonlocal elasticity for nonlinear vibration characteristics of carbon/boron-nitride hetero-nanotube subject to magneto-thermal environment. *Phys. Scr.* **2020**, *95*, 055218. [CrossRef]
31. Farajpour, A.; Howard, C.Q.; Robertson, W.S.P. On size-dependent mechanics of nanoplates. *Int. J. Eng. Sci.* **2020**, *156*, 103368. [CrossRef]
32. Barretta, R.; Fabbrocino, F.; Luciano, R.; Marotti de Sciarra, F. Closed-form solutions in stress-driven two-phase integral elasticity for bending of functionally graded nano-beams. *Phys. E Low-Dimens. Syst. Nanostructures* **2018**, *97*, 13–30. [CrossRef]
33. Vaccaro, M.S.; Pinnola, F.P.; Marotti de Sciarra, F.; Čanađija, M.; Barretta, R. Stress-driven two-phase integral elasticity for Timoshenko curved beams. *Proc. Inst. Mech. Eng. Part N J. Nanomater. Nanoeng. Nanosyst.* **2021**, *235*, 52–63. [CrossRef]
34. Zhang, P.; Qing, H.; Gao, C.F. Exact solutions for bending of Timoshenko curved nanobeams made of functionally graded materials based on stress-driven nonlocal integral model. *Compos. Struct.* **2020**, *245*, 112362. [CrossRef]
35. Vaccaro, M.S.; Sedighi, H.M. Two-phase elastic axisymmetric nanoplates. *Eng. Comput.* **2022**, *in press*. [CrossRef]
36. Farajpour, A.; Ghayesh, M.H.; Farokhi, H. A review on the mechanics of nanostructures. *Int. J. Eng. Sci.* **2018**, *133*, 231–263. [CrossRef]
37. Shariati, M.; Shishesaz, M.; Sahbafar, H.; Pourabdy, M.; Hosseini, M. A review on stress-driven nonlocal elasticity theory. *J. Comput. Appl. Mech.* **2021**, *52*, 535–552.
38. Rogula, D. Introduction to nonlocal theory of material media. In *Nonlocal Theory of Material Media*; Rogula, D., Ed.; Springer: Vienna, Austria, 1982; pp. 123–222.
39. Krumhansl, J.A. Some considerations of the relation between solid state physics and generalized continuum mechanics. In *Proceedings of the Mechanics of Generalized Continua*; Kröner, E., Ed.; Springer: Berlin/Heidelberg, Germany, 1968; pp. 298–311.
40. Kunin, I.A. The theory of elastic media with microstructure and the theory of dislocations. In *Proceedings of the Mechanics of Generalized Continua*; Kröner, E., Ed.; Springer: Berlin/Heidelberg, Germany, 1968; pp. 321–329.
41. Romano, G.; Luciano, R.; Barretta, R.; Diaco, M. Nonlocal integral elasticity in nanostructures, mixtures, boundary effects and limit behaviours. *Contin. Mech. Thermodyn.* **2018**, *30*, 641–655. [CrossRef]
42. Benvenuti, E.; Simone, A. One-dimensional nonlocal and gradient elasticity: Closed-form solution and size effect. *Mech. Res. Commun.* **2013**, *48*, 46–51. [CrossRef]
43. Vaccaro, M.S.; Barretta, R.; Marotti de Sciarra, F.; Reddy, J.N. Nonlocal integral elasticity for third-order small-scale beams. *Acta Mech.* **2022**, *233*, 2393–2403. [CrossRef]
44. Fernández-Sáez, J.; Zaera, R.; Loya, J.; Reddy, J. Bending of Euler–Bernoulli beams using Eringen's integral formulation: A paradox resolved. *Int. J. Eng. Sci.* **2016**, *99*, 107–116. [CrossRef]
45. Romano, G.; Barretta, R.; Diaco, M.; Marotti de Sciarra, F. Constitutive boundary conditions and paradoxes in nonlocal elastic nanobeams. *Int. J. Mech. Sci.* **2017**, *121*, 151–156. [CrossRef]
46. Zhu, X.; Wang, Y.; Dai, H.H. Buckling analysis of Euler–Bernoulli beams using Eringen's two-phase nonlocal model. *Int. J. Eng. Sci.* **2017**, *116*, 130–140. [CrossRef]
47. Zhang, P.; Qing, H. Free vibration analysis of Euler–Bernoulli curved beams using two-phase nonlocal integral models. *J. Vib. Control.* **2021**, *28*, 2861–2878. [CrossRef]

48. Naghinejad, M.; Ovesy, H.R. Nonlinear post-buckling analysis of viscoelastic nano-scaled beams by nonlocal integral finite element method. *ZAMM J. Appl. Math. Mech./Z. für Angew. Math. Und Mech.* **2022**, *102*, e202100148. [CrossRef]
49. Providas, E. Closed-Form Solution of the Bending Two-Phase Integral Model of Euler-Bernoulli Nanobeams. *Algorithms* **2022**, *15*, 151. [CrossRef]
50. Zhang, P.; Qing, H. Closed-form solution in bi-Helmholtz kernel based two-phase nonlocal integral models for functionally graded Timoshenko beams. *Compos. Struct.* **2021**, *265*, 113770. [CrossRef]
51. Tricomi, F.G. *Integral Equations*; Interscience: New York, NY, USA, 1957.
52. Polyanin, P.; Manzhirov, A. *Handbook of Integral Equations*, 2nd ed.; Chapman and Hall/CRC: Boca Raton, FL, USA, 2008.
53. Romano, G.; Diaco, M. On formulation of nonlocal elasticity problems. *Meccanica* **2020**, *56*, 1303–1328. [CrossRef]
54. Pisano, A.A.; Fuschi, P.; Polizzotto, C. Integral and differential approaches to Eringen's nonlocal elasticity models accounting for boundary effects with applications to beams in bending. *ZAMM J. Appl. Math. Mech./Z. für Angew. Math. Und Mech.* **2021**, *101*, e202000152. [CrossRef]
55. Pisano, A.A.; Fuschi, P.; Polizzotto, C. Euler–Bernoulli elastic beam models of Eringen's differential nonlocal type revisited within a C^0-continuous displacement framework. *Meccanica* **2021**, *56*, 2323–2337. [CrossRef]
56. Barretta, R.; Faghidian, S.A.; Marotti de Sciarra, F. Stress-driven nonlocal integral elasticity for axisymmetric nano-plates. *Int. J. Eng. Sci.* **2019**, *136*, 38–52. [CrossRef]
57. Oskouie, M.F.; Ansari, R.; Rouhi, H. Bending of Euler-Bernoulli nanobeams based on the strain- and stress-driven nonlocal integral models: A numerical approach. *Acta Mech. Sin.* **2018**, *34*, 871–882. [CrossRef]
58. Oskouie, M.F.; Ansari, R.; Rouhi, H. A numerical study on the buckling and vibration of nanobeams based on the strain- and stress-driven nonlocal integral models. *Int. J. Comput. Mater. Sci. Eng.* **2018**, *7*, 1850016.
59. Barretta, R.; Faghidian, S.A.; Luciano, R. Longitudinal vibrations of nano-rods by stress-driven integral elasticity. *Mech. Adv. Mater. Struct.* **2019**, *26*, 1307–1315. [CrossRef]
60. Qing, H.; Wei, L. Linear and nonlinear free vibration analysis of functionally graded porous nanobeam using stress-driven nonlocal integral model. *Commun. Nonlinear Sci. Numer. Simul.* **2022**, *109*, 106300. [CrossRef]
61. Mahmoudpour, E.; Esmaeili, M. Nonlinear free and forced vibration of carbon nanotubes conveying magnetic nanoflow and subjected to a longitudinal magnetic field using stress-driven nonlocal integral model. *Thin-Walled Struct.* **2021**, *166*, 108134. [CrossRef]
62. Darban, H.; Luciano, R.; Darban, R. Buckling of cracked micro- and nanocantilevers. *Acta Mech.* **2022**, *234*, 693–704. [CrossRef]
63. Abazari, A.M.; Safavi, S.M.; Rezazadeh, G.; Villanueva, L.G. Modelling the Size Effects on the Mechanical Properties of Micro/Nano Structures. *Sensors* **2015**, *15*, 28543–28562. [CrossRef]
64. Lam, D.C.C.; Yang, F.; Chong, A.C.M.; Wang, J.; Tong, P. Experiments and theory in strain gradient elasticity. *J. Mech. Phys. Solids* **2003**, *51*, 1477–1508. [CrossRef]
65. Zarepour, M.; Hosseini, S.; Akbarzadeh, A. Geometrically nonlinear analysis of Timoshenko piezoelectric nanobeams with flexoelectricity effect based on Eringen's differential model. *Appl. Math. Model.* **2019**, *69*, 563–582. [CrossRef]
66. Gholipour, A.; Ghayesh, M.H. Nonlinear coupled mechanics of functionally graded nanobeams. *Int. J. Eng. Sci.* **2020**, *150*, 103221. [CrossRef]
67. Ghaffari, S.S.; Ceballes, S.; Abdelkefi, A. Nonlinear dynamical responses of forced carbon nanotube-based mass sensors under the influence of thermal loadings. *Nonlinear Dyn.* **2020**, *100*, 1013–1035. [CrossRef]
68. Gholami, M.; Zare, E.; Alibazi, A. Applying Eringen's nonlocal elasticity theory for analyzing the nonlinear free vibration of bidirectional functionally graded Euler–Bernoulli nanobeams. *Arch. Appl. Mech.* **2021**, *91*, 2957–2971. [CrossRef]
69. Saadatmand, M.; Shahabodini, A.; Ahmadi, B.; Chegini, S. Nonlinear forced vibrations of initially curved rectangular single layer graphene sheets: An analytical approach. *Phys. E Low-Dimens. Syst. Nanostructures* **2021**, *127*, 114568. [CrossRef]
70. Lanzoni, L.; Tarantino, A.M. Bending of nanobeams in finite elasticity. *Int. J. Mech. Sci.* **2021**, *202-203*, 106500. [CrossRef]
71. Karimipour, I.; Beni, Y.T. Nonlinear dynamic analysis of nonlocal composite laminated toroidal shell segments subjected to mechanical shock. *Commun. Nonlinear Sci. Numer. Simul.* **2022**, *106*, 106105. [CrossRef]
72. Jin, Q.; Ren, Y. Nonlinear size-dependent bending and forced vibration of internal flow-inducing pre- and post-buckled FG nanotubes. *Commun. Nonlinear Sci. Numer. Simul.* **2022**, *104*, 106044. [CrossRef]
73. Alibakhshi, A.; Dastjerdi, S.; Fantuzzi, N.; Rahmanian, S. Nonlinear free and forced vibrations of a fiber-reinforced dielectric elastomer-based microbeam. *Int. J. -Non-Linear Mech.* **2022**, *144*. [CrossRef]
74. Tang, Y.; Qing, H. Size-dependent nonlinear post-buckling analysis of functionally graded porous Timoshenko microbeam with nonlocal integral models. *Commun. Nonlinear Sci. Numer. Simul.* **2023**, *116*, 106808. [CrossRef]
75. Mamandi, A. Nonlocal large deflection analysis of a cantilever nanobeam on a nonlinear Winkler-Pasternak elastic foundation and under uniformly distributed lateral load. *J. Mech. Sci. Technol.* **2023**, *37*, 813–824. [CrossRef]
76. Malikan, M.; Wiczenbach, T.; Eremeyev, V. Thermal buckling of functionally graded piezomagnetic micro- and nanobeams presenting the flexomagnetic effect. *Contin. Mech. Thermodyn.* **2022**, *34*, 1051–1066. [CrossRef]
77. Vaccaro, M.S. On geometrically nonlinear mechanics of nanocomposite beams. *Int. J. Eng. Sci.* **2022**, *173*, 103653. [CrossRef]
78. Chen, L. An integral approach for large deflection cantilever beams. *Int. J. -Non-Linear Mech.* **2010**, *45*, 301–305. [CrossRef]
79. Reddy, J.N. A simple higher-order theory for laminated composite plates. *J. Appl. Mech.* **1984**, *51*, 745–752. [CrossRef]

80. Reddy, J.N.; Wang, C.M.; Lee, K.H. Relationships between bending solutions of classical and shear deformation beam theories. *Int. J. Solids Struct.* **1997**, *34*, 3373–3384. [CrossRef]
81. Heyliger, P.R.; Reddy, J.N. A higher-order beam finite element for bending and vibration problems. *J. Sound Vib.* **1988**, *126*, 309–326. [CrossRef]
82. Reddy, J.N. *Theories and Analyses of Beams and Axisymmetric Circular Plates*; Taylor & Francis (CRC Press): Philadelphia, PA, USA, 2022.
83. Levinson, M. A new rectangular beam theory. *J. Sound Vib.* **1981**, *74*, 81–87. [CrossRef]
84. Bickford, W.B. A consistent higher order beam theory. *Dev. Theor. Appl. Mech.* **1982**, *11*, 137–150.
85. Reddy, J.N. *Energy Principles and Variational Methods in Applied Mechanics*, 2nd ed.; John Wiley & Sons: New York, NY, USA, 2002.
86. Jankowski, P.; Żur, K.K.; Kim, J.; Reddy, J. On the bifurcation buckling and vibration of porous nanobeams. *Compos. Struct.* **2020**, *250*, 112632. [CrossRef]
87. Barretta, R.; Luciano, R.; Marotti de Sciarra, F.; Ruta, G. Stress-driven nonlocal integral model for Timoshenko elastic nano-beams. *Eur. J. Mech. A/Solids* **2018**, *72*, 275–286. [CrossRef]
88. Zhang, P.; Qing, H. On well-posedness of two-phase nonlocal integral models for higher-order refined shear deformation beams. *Appl. Math. Mech.* **2021**, *42*, 931–950. [CrossRef]
89. Vantadori, S.; Luciano, R.; Scorza, D.; Darban, H. Fracture analysis of nanobeams based on the stress-driven non-local theory of elasticity. *Mech. Adv. Mater. Struct.* **2022**, *29*, 1967–1976. [CrossRef]
90. Zhang, P.; Schiavone, P.; Qing, H. Unified two-phase nonlocal formulation for vibration of functionally graded beams resting on nonlocal viscoelastic Winkler-Pasternak foundation. *Appl. Math. Mech.-Engl.* **2022**, *44*, 89–108. [CrossRef]
91. Scorza, D.; Luciano, R.; Vantadori, S. Fracture behaviour of nanobeams through Two-Phase Local/Nonlocal Stress-Driven model. *Compos. Struct.* **2022**, *280*, 114957. [CrossRef]
92. Rezaiee-Pajand, M.; Rajabzadeh-Safaei, N. Stress-driven nonlinear behavior of curved nanobeams. *Int. J. Eng. Sci.* **2022**, *178*, 103724. [CrossRef]
93. Xu, X.; Karami, B.; Shahsavari, D. Time-dependent behavior of porous curved nanobeam. *Int. J. Eng. Sci.* **2021**, *160*, 103455. [CrossRef]
94. Karamanli, A.; Vo, T.P. Finite element model for free vibration analysis of curved zigzag nanobeams. *Compos. Struct.* **2022**, *282*, 115097. [CrossRef]
95. Bacciocchi, M.; Tarantino, A.M. Analytical solutions for vibrations and buckling analysis of laminated composite nanoplates based on third-order theory and strain gradient approach. *Compos. Struct.* **2021**, *272*, 114083. [CrossRef]
96. Bacciocchi, M.; Fantuzzi, N.; Neves, A.; Ferreira, A. Vibrations and bending of thin laminated square plates with holes in gradient elasticity: A finite element solution. *Mech. Res. Commun.* **2023**, *128*. [CrossRef]
97. Lin, M.X.; Chen, C. Investigation of pull-in behavior of circular nanoplate actuator based on the modified couple stress theory. *Eng. Comput.* **2020**, *38*, 2648–2665. [CrossRef]
98. Furletov, A.; Apyari, V.; Garshev, A.; Dmitrienko, S.; Zolotov, Y. Fast and Sensitive Determination of Bioflavonoids Using a New Analytical System Based on Label-Free Silver Triangular Nanoplates. *Sensors* **2022**, *22*, 843. [CrossRef]
99. Fernández-Sáez, J.; Morassi, A.; Rubio, L.; Zaera, R. Transverse free vibration of resonant nanoplate mass sensors: Identification of an attached point mass. *Int. J. Mech. Sci.* **2019**, *150*, 217–225. [CrossRef]
100. Farajpour, A.; Żur, K.K.; Kim, J.; Reddy, J. Nonlinear frequency behaviour of magneto-electromechanical mass nanosensors using vibrating MEE nanoplates with multiple nanoparticles. *Compos. Struct.* **2021**, *260*, 113458. [CrossRef]
101. Chenghui, X.; Qu, J.; Rong, D.; Zhou, Z.; Leung, A. Theory and modeling of a novel class of nanoplate-based mass sensors with corner point supports. *Thin-Walled Struct.* **2021**, *159*, 107306.
102. Zhou, H.; Shao, D.; Song, X.; Li, P. Three-dimensional thermoelastic damping models for rectangular micro/nanoplate resonators with nonlocal-single-phase-lagging effect of heat conduction. *Int. J. Heat Mass Transf.* **2022**, *196*, 123271. [CrossRef]
103. Pham, Q.H.; Tran, T.T.; Nguyen, P.C. Nonlocal free vibration of functionally graded porous nanoplates using higher-order isogeometric analysis and ANN prediction. *Alex. Eng. J.* **2023**, *66*, 651–667. [CrossRef]
104. Al-Furjan, M.; Shan, L.; Shen, X.; Kolahchi, R.; Rajak, D.K. Combination of FEM-DQM for nonlinear mechanics of porous GPL-reinforced sandwich nanoplates based on various theories. *Thin-Walled Struct.* **2022**, *178*, 109495. [CrossRef]
105. Kawano, A.; Morassi, A.; Zaera, R. Inverse load identification in vibrating nanoplates. *Math. Methods Appl. Sci.* **2023**, *46*, 1045–1075. [CrossRef]
106. Pinnola, F.P.; Vaccaro, M.S.; Barretta, R.; Marotti de Sciarra, F. Random vibrations of stress-driven nonlocal beams with external damping. *Meccanica* **2021**, *56*, 1329–1344. [CrossRef]
107. Shinozuka, M.; Deodatis, G. Stochastic process models for earthquake ground motion. *Probabilistic Eng. Mech.* **1988**, *3*, 114–123. [CrossRef]
108. Dilena, M.; Fedele Dell'Oste, M.; Fernández-Sáez, J.; Morassi, A.; Zaera, R. Hearing distributed mass in nanobeam resonators. *Int. J. Solids Struct.* **2020**, *193*, 568–592. [CrossRef]
109. Alibakhshi, A.; Dastjerdi, S.; Malikan, M.; Eremeyev, V. Nonlinear free and forced vibrations of a dielectric elastomer-based microcantilever for atomic force microscopy. *Contin. Mech. Thermodyn.* **2022**, *in press*. [CrossRef]
110. Nguyen, P.C.; Pham, Q.H. A nonlocal isogeometric model for buckling and dynamic instability analyses of FG graphene platelets-reinforced nanoplates. *Mater. Today Commun.* **2023**, *34*, 105211. [CrossRef]

111. Zhang, Q.; Li, M.; Zhao, M. Dynamic analysis of a piezoelectric semiconductor nanoplate with surface effect. *Mater. Today Commun.* **2022**, *33*, 104406. [CrossRef]
112. Gusella, V.; Autuori, G.; Pucci, P.; Cluni, F. Dynamics of Nonlocal Rod by Means of Fractional Laplacian. *Symmetry* **2020**, *12*, 1933. [CrossRef]
113. Darban, H.; Luciano, R.; Basista, M. Free transverse vibrations of nanobeams with multiple cracks. *Int. J. Eng. Sci.* **2022**, *177*, 103703. [CrossRef]
114. Corigliano, A.; Ardito, R.; Comi, C.; Ghisi, A.; Mariani, S. *Mechanics of Microsystems*; John Wiley & Sons, Ltd.: Hoboken, NJ, USA, 2018. [CrossRef]
115. Jalaei, M.; Thai, H.T.; Civalek, O. On viscoelastic transient response of magnetically imperfect functionally graded nanobeams. *Int. J. Eng. Sci.* **2022**, *172*, 103629. [CrossRef]
116. Akgöz, B.; Civalek, O. Buckling Analysis of Functionally Graded Tapered Microbeams via Rayleigh–Ritz Method. *Mathematics* **2022**, *10*, 4429. [CrossRef]
117. Comi, C.; Corigliano, A.; Frangi, A.; Zega, V. Linear and nonlinear mechanics in MEMS; In *Silicon Sensors and Actuators: The Feynman Roadmap*; Springer: Cham, Switzerland, 2022; pp. 389–437. [CrossRef]
118. Numanouglu, H.M.; Ersoy, H.; Akgöz, B.; Civalek, O. A new eigenvalue problem solver for thermo-mechanical vibration of Timoshenko nanobeams by an innovative nonlocal finite element method. *Math. Methods Appl. Sci.* **2022**, *45*, 2592–2614. [CrossRef]
119. Civalek, O.; Uzun, B.; Yayli, M.; Akgöz, B. Size-dependent transverse and longitudinal vibrations of embedded carbon and silica carbide nanotubes by nonlocal finite element method. *Eur. Phys. J. Plus* **2020**, *135*, 381. [CrossRef]
120. Ebrahimi, F.; Barati, M.; Civalek, O. Application of Chebyshev–Ritz method for static stability and vibration analysis of nonlocal microstructure-dependent nanostructures. *Eng. Comput.* **2020**, *36*. [CrossRef]
121. Żur, K.K.; Farajpour, A.; Lim, C.; Jankowski, P. On the nonlinear dynamics of porous composite nanobeams connected with fullerenes. *Compos. Struct.* **2021**, *274*, 114356. [CrossRef]
122. Vaccaro, M.S.; Marotti de Sciarra, F.; Barretta, R. On the regularity of curvature fields in stress-driven nonlocal elastic beams. *Acta Mech.* **2021**, *232*, 2595–2603. [CrossRef]
123. Caporale, A.; Darban, H.; Luciano, R. Exact closed-form solutions for nonlocal beams with loading discontinuities. *Mech. Adv. Mater. Struct.* **2022**, *29*, 694–704. [CrossRef]
124. Pinnola, F.; Vaccaro, M.S.; Barretta, R.; Marotti de Sciarra, F. Finite element method for stress-driven nonlocal beams. *Eng. Anal. Bound. Elem.* **2022**, *134*, 22–34. [CrossRef]
125. Scorza, D.; Vantadori, S.; Luciano, R. Nanobeams with Internal Discontinuities: A Local/Nonlocal Approach. *Nanomaterials* **2021**, *11*, 2651. [CrossRef]
126. Caporale, A.; Darban, H.; Luciano, R. Nonlocal strain and stress gradient elasticity of Timoshenko nano-beams with loading discontinuities. *Int. J. Eng. Sci.* **2022**, *173*, 103620. [CrossRef]
127. Togun, N.; Bagdatli, S.M. Nonlinear Vibration of a Nanobeam on a Pasternak Elastic Foundation Based on Non-Local Euler-Bernoulli Beam Theory. *Math. Comput. Appl.* **2016**, *21*, 3. [CrossRef]
128. Togun, N. Nonlocal beam theory for nonlinear vibrations of a nanobeam resting on elastic foundation. *Bound. Value Probl.* **2016**, *2016*, 57. [CrossRef]
129. Ebrahimi, F.; Barati, M.R. Buckling analysis of nonlocal third-order shear deformable functionally graded piezoelectric nanobeams embedded in elastic medium. *J. Braz. Soc. Mech. Sci. Eng.* **2017**, *39*, 937–952. [CrossRef]
130. Darban, H.; Fabbrocino, F.; Feo, L.; Luciano, R. Size-dependent buckling analysis of nanobeams resting on two-parameter elastic foundation through stress-driven nonlocal elasticity model. *Mech. Adv. Mater. Struct.* **2021**, *28*, 2408–2416. [CrossRef]
131. Mahmoudpour, E.; Hosseini-Hashemi, S.H.; Faghidian, S.A. Nonlinear vibration analysis of FG nano-beams resting on elastic foundation in thermal environment using stress-driven nonlocal integral model. *Appl. Math. Model.* **2018**, *57*, 302–315. [CrossRef]
132. Uzun, B.; Civalek, O. Free vibration analysis Silicon nanowires surrounded by elastic matrix by nonlocal finite element method. *Adv. Nano Res.* **2019**, *7*, 99–108.
133. Koutsoumaris, C.; Eptaimeros, K. Nonlocal integral static problems of nanobeams resting on an elastic foundation. *Eur. J. Mech. A/Solids* **2021**, *89*, 104295. [CrossRef]
134. Adhikari, S.; Karlicic, D.; Liu, X. Dynamic stiffness of nonlocal damped nano-beams on elastic foundation. *Eur. J. Mech. / A Solids* **2021**, *86*, 4. [CrossRef]
135. Tran, T.T.; Tran, V.K.; Pham, Q.H.; Zenkour, A.M. Extended four-unknown higher-order shear deformation nonlocal theory for bending, buckling and free vibration of functionally graded porous nanoshell resting on elastic foundation. *Compos. Struct.* **2021**, *264*, 113737. [CrossRef]
136. Pham, Q.H.; Tran, V.K.; Tran, T.T.; Nguyen, P.C.; Malekzadeh, P. Dynamic instability of magnetically embedded functionally graded porous nanobeams using the strain gradient theory. *Alex. Eng. J.* **2022**, *61*, 10025–10044. [CrossRef]
137. Jena, S.; Chakraverty, S.; Mahesh, V.; Harursampath, D.; Sedighi, H.M. A Novel Numerical Approach for the Stability of Nanobeam Exposed to Hygro-Thermo-Magnetic Environment Embedded in Elastic Foundation. *ZAMM J. Appl. Math. Mech./Z. für Angew. Math. Und Mech.* **2022**, *102*, e202100380. [CrossRef]
138. Darban, H.; Luciano, R.; Caporale, A.; Basista, M. Modeling of buckling of nanobeams embedded in elastic medium by local-nonlocal stress-driven gradient elasticity theory. *Compos. Struct.* **2022**, *297*, 115907. [CrossRef]

139. Barretta, R.; Čanađija, M.; Luciano, R.; Marotti de Sciarra, F. On the mechanics of nanobeams on nano-foundations. *Int. J. Eng. Sci.* **2022**, *180*, 103747. [CrossRef]
140. Vaccaro, M.S.; Pinnola, F.P.; Marotti de Sciarra, F.; Barretta, R. Elastostatics of Bernoulli–Euler Beams Resting on Displacement-Driven Nonlocal Foundation. *Nanomaterials* **2021**, *11*, 573. [CrossRef]
141. Wieghardt, K. Über den Balken auf nachgiebiger Unterlage. *ZAMM - J. Appl. Math. Mech./ Z. für Angew. Math. Und Mech.* **1922**, *2*, 165–184. [CrossRef]
142. Sollazzo, A. Equilibrio della trave su suolo di Wieghardt. *Tec. Ital.* **1966**, *31*, 187–206.